Pressure Effects on Mechanical Behavior and Deformation Processing of Materials

John J. Lewandowski
Department of Materials Science and Engineering
Case Western Reserve University
Cleveland, Ohio 44106-7204

August 3, 2015

IMS
Institute for Materials Science
Los Alamos

Acknowledgements

Visit Sponsorship: LANL Institute for Materials Science

Research Funding:

NSF-PYI	ALCOA
NSF-DMR	DARPA
AFOSR	Boeing
ONR	Pratt & Whitney
ARO	NASA Glenn
ALCAN	LANL

Students/Collaborators:

AL Grow, Y Esmaelipour, A Vaidya, P Lowhaphandu, J Larose, P Wesseling, JB Caris, S Solv'yev, G Sunny, DS Liu, RW Margevicius, FP Yuan, PM Singh, SN Patankar, BC Ko, LO Vatamanu, J Bobanga, E Aydogan

JD Embury, O Richmond, V Prakash, R Ballarini, WH Hunt, IE Locci, RD Noebe, BA Lerch, GT Gray III, TE Mitchell, I Anderson, SA Maloy, R Odette

IMS Institute for Materials Science Los Alamos

Review Paper: J.J. Lewandowski and P. Lowhaphandu, "Effects of Hydrostatic Pressure on Mechanical Behavior and Deformation Processing of Materials", International Materials Reviews, 43(4), pp. 145-188, 1988.

Outline

- High Pressure Testing Rigs
  - Pressure Media: Gas, Oil
  - Internal Load Cell, Pressure Measurement
- Pressure Effects on Flow of Metallic Alloys
  - Yielding
    - Cubic Systems
    - Non-Cubic Systems
    - Particle-containing systems
  - UTS

- Pressure Effects on Fracture of Metallic Alloys
    - Fracture Micro-mechanisms
    - Pressure Effects on Ductility/Fracture
- Pressure Effects on Composites, Intermetallics
  - Flow
    - Ductility/Fracture
    - Pressure and Temperature Effects
        - Implications on Deformation Processing
- Hydrostatic Extrusion
    - Concept
    - Examples (Composites, NiAl)
    - ODS Tubes?
        - Billet Design, Initial Results

IMS
Institute for Materials Science
Los Alamos

Superimposed Pressure Testing

High Pressure Deformation Apparatus

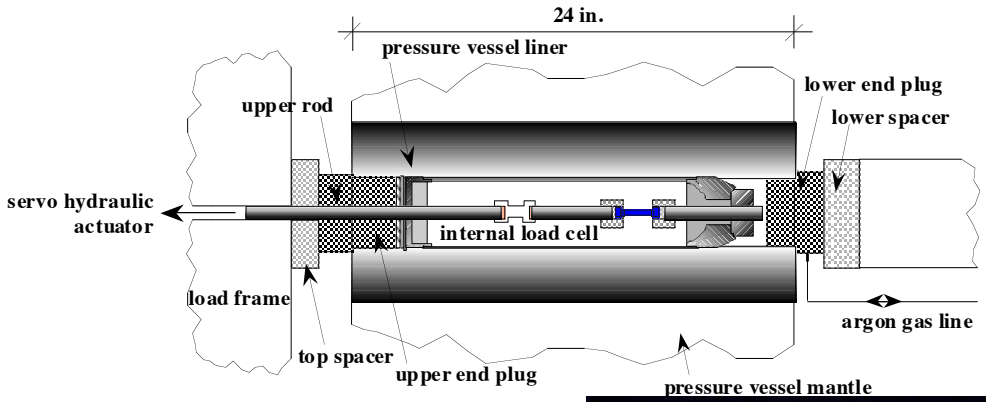

- max. pressure: 700 MPa
- strain rate: 10^{-6} to 10^{2} s^{-1}
- pressurizing medium: Ar
- internal/external load cell
- LVDT/strain gage

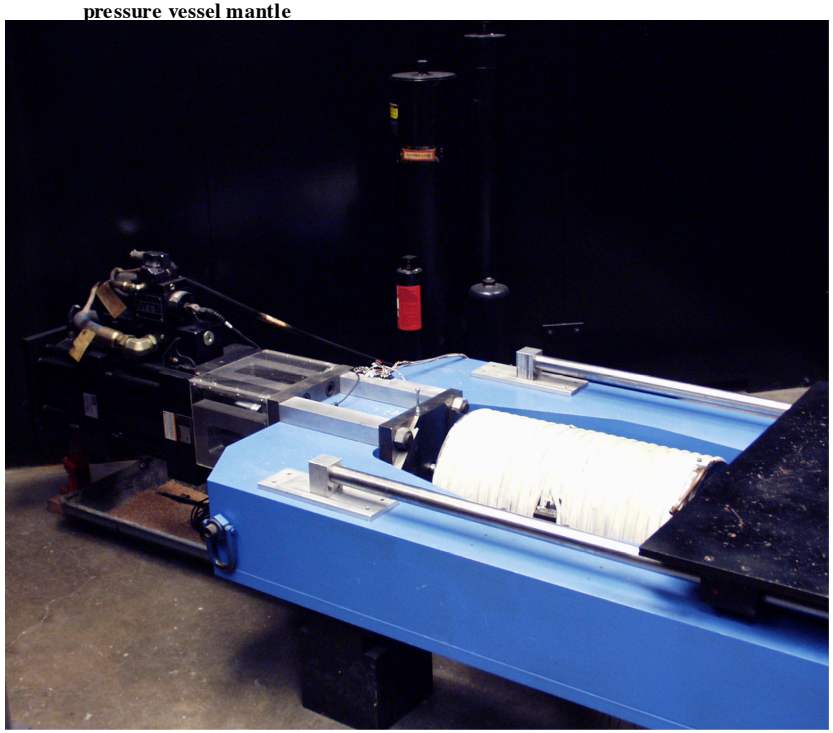

IMS Institute for Materials Science Los Alamos

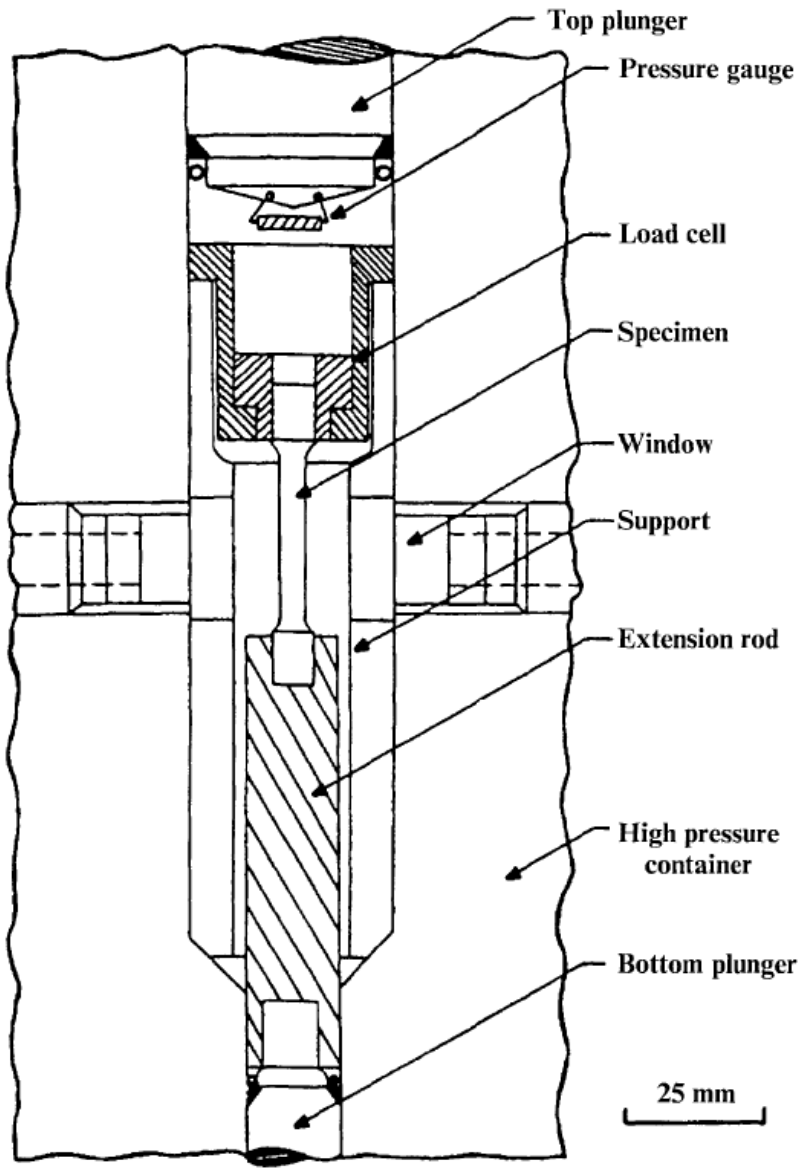

1 Schematic diagram of oil based high pressure deformation apparatus[36,72,122,126,269,326–329]

J.J. Lewandowski and P. Lowhaphandu, International Materials Reviews, Vol.43, No.4, 1998.

Effects of Hydrostatic Pressure on Yield Strength

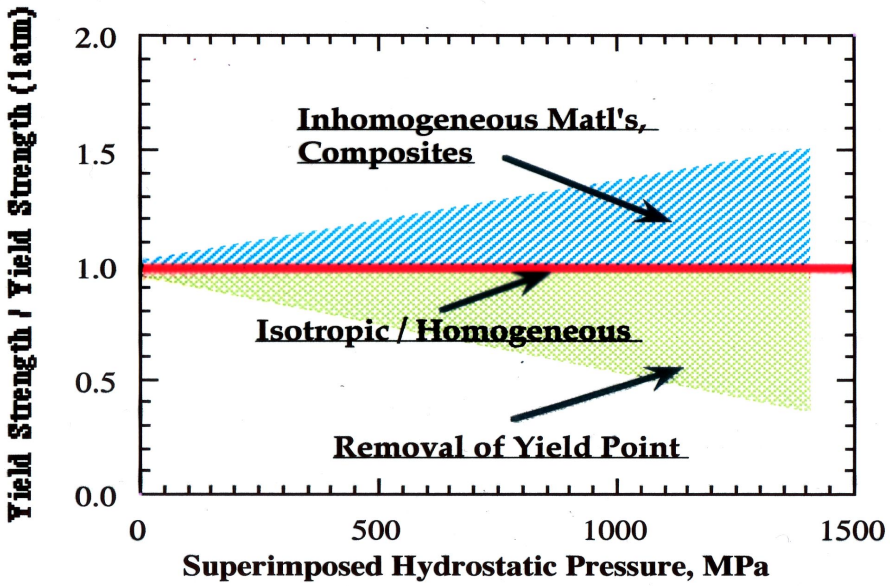

I. Isotropic/Homogenous Materials

Hydrostatic pressure has no effect on yield strength as predicted by various yield criterion, e.g. the von Mises yield criterion

$$\sigma_y = \frac{1}{\sqrt{2}}\left[(\sigma_1-\sigma_2)^2+(\sigma_2-\sigma_3)^2+(\sigma_3-\sigma_1)^2\right]^{1/2}$$

Ex. Steels, Al alloys, Pure cubic metals

II. Inhomogeneous Materials

i) Removal of yield point: For materials that exhibit a removal of yield point due to pressure-induced generation of mobile dislocations, the yield strength generally decreases with increasing pressure.
Ex. Fe, Cr, W, NiAl

ii) Composites/Other inhomogeneous systems:
The increase in yield strength with pressure is due to the generation of dislocations at the reinforcement/matrix interfaces and due to the suppression of damage associated with the reinforcement in composites. Relaxation of residual stress and decreased constraint may reduce the flow stress.
Ex. 6061Al-Al_2O_3, AZ91-SiCp, Cd, Zn

IMS Institute for Materials Science Los Alamos

Ref.: J.J. Lewandowski and P. Lowhaphandu, International Materials Reviews, Vol.43, No.4, 1998.

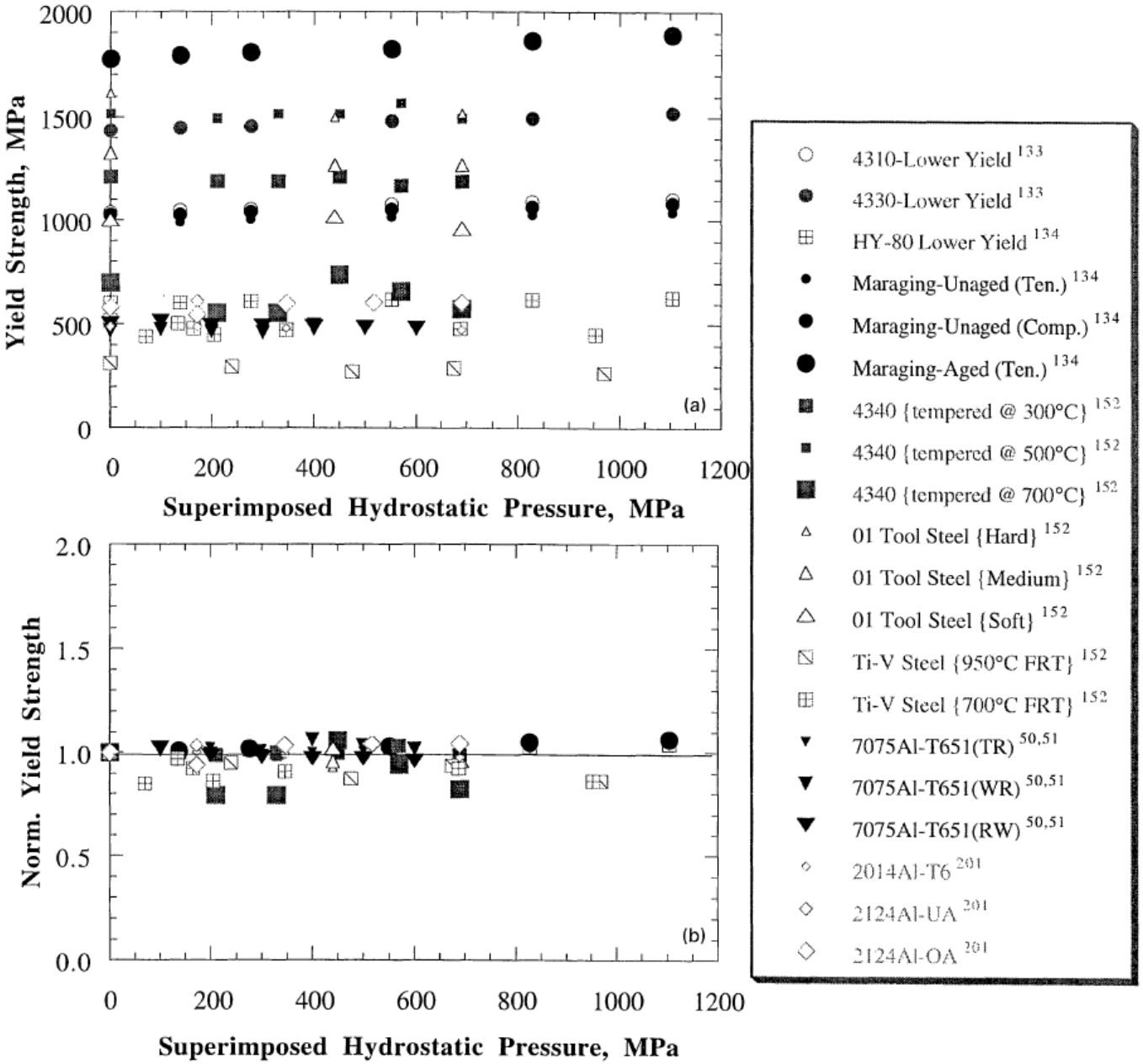

a yield strength *v.* superimposed hydrostatic pressure; *b* normalised yield strength *v.* superimposed hydrostatic pressure

5 Effect of pressure on yield strength of various bcc and fcc metallic alloys

J.J. Lewandowski and P. Lowhaphandu, International Materials Reviews, Vol.43, No.4, 1998.

IMS Institute for Materials Science Los Alamos

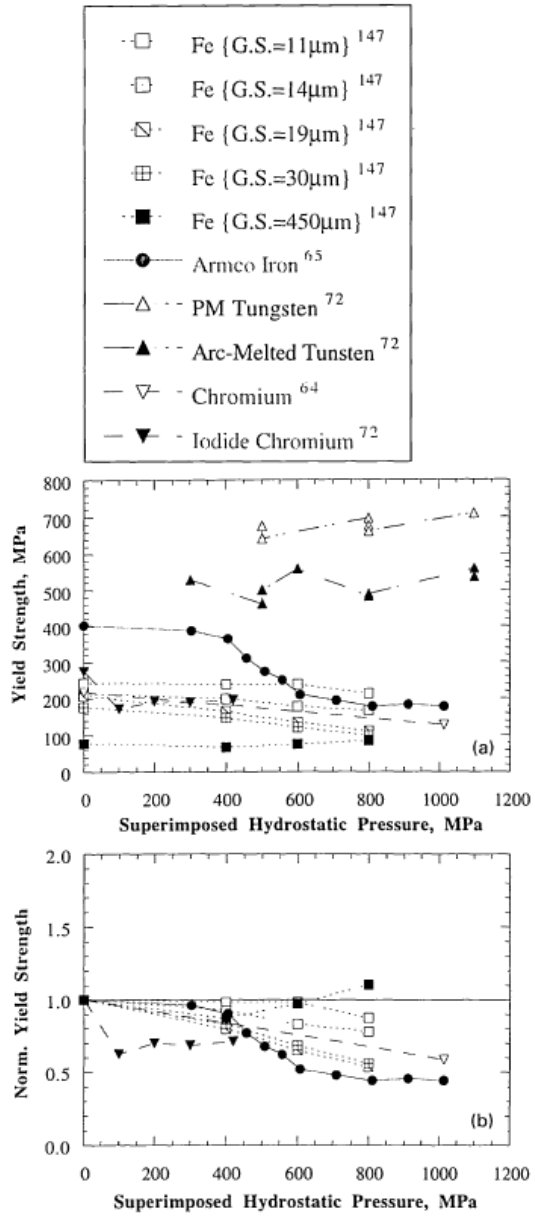

a yield strength *v.* superimposed hydrostatic pressure; *b* normalised yield strength *v.* superimposed hydrostatic pressure

6 Effect of pressure on yield strength of various bcc metals; G.S. grain size

IMS Institute for Materials Science Los Alamos

J.J. Lewandowski and P. Lowhaphandu, International Materials Reviews, Vol.43, No.4, 1998.

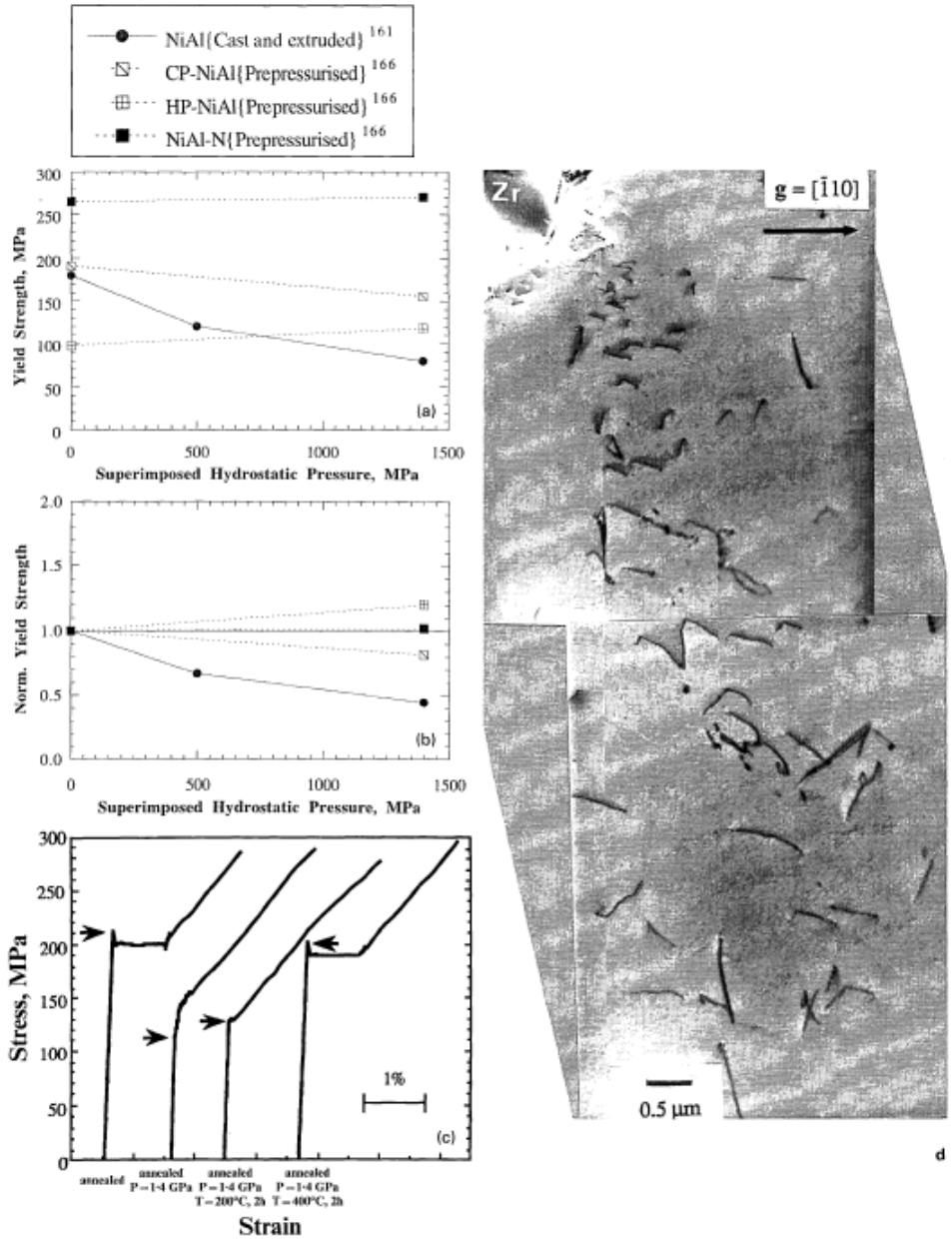

a yield strength *v.* superimposed hydrostatic pressure; *b* normalised yield strength *v.* superimposed hydrostatic pressure; *c* stress–strain curves of polycrystalline NiAl tested in tension after annealing at 827°C for 2 h, pressurised to 1·4 GPa, and tested at atmospheric pressure, and after aging pressurised specimens at either 200°C or 400°C for 2 h (Ref. 159) (arrows show proportional limit); *d* dislocations being punched from Zr inclusion in NiAl pressurised to 1·4 GPa (Refs. 156, 157, 160, 161)

7 Effect of pressure on yield strength of NiAl

IMS Institute for Materials Science Los Alamos

J.J. Lewandowski and P. Lowhaphandu, International Materials Reviews, Vol.43, No.4, 1998.

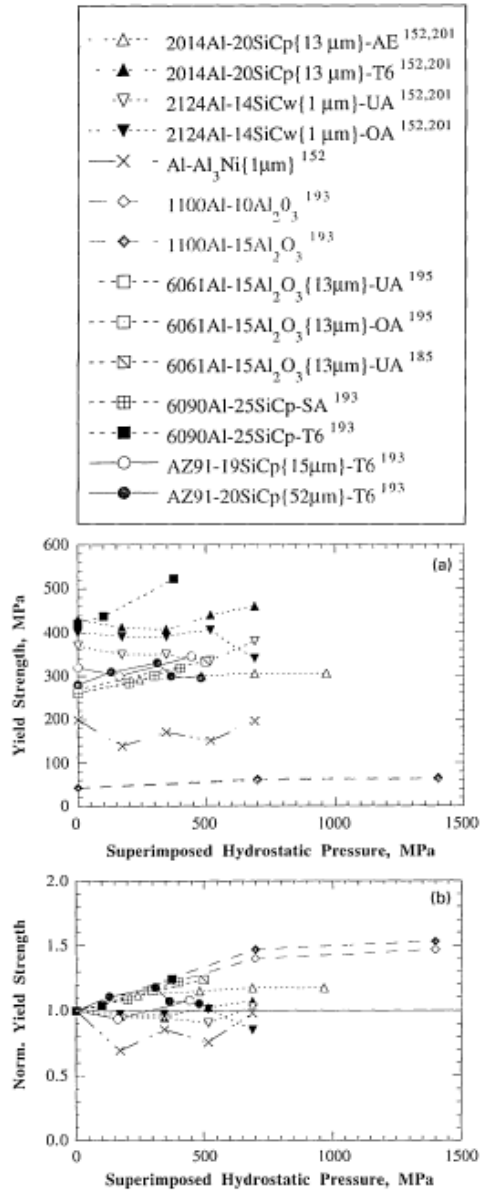

a yield strength *v.* superimposed hydrostatic pressure; *b* normalised yield strength *v.* superimposed hydrostatic pressure

8 Effect of pressure on yield strength of discontinuously reinforced metal matrix composites

J.J. Lewandowski and P. Lowhaphandu, International Materials Reviews, Vol.43, No.4, 1998.

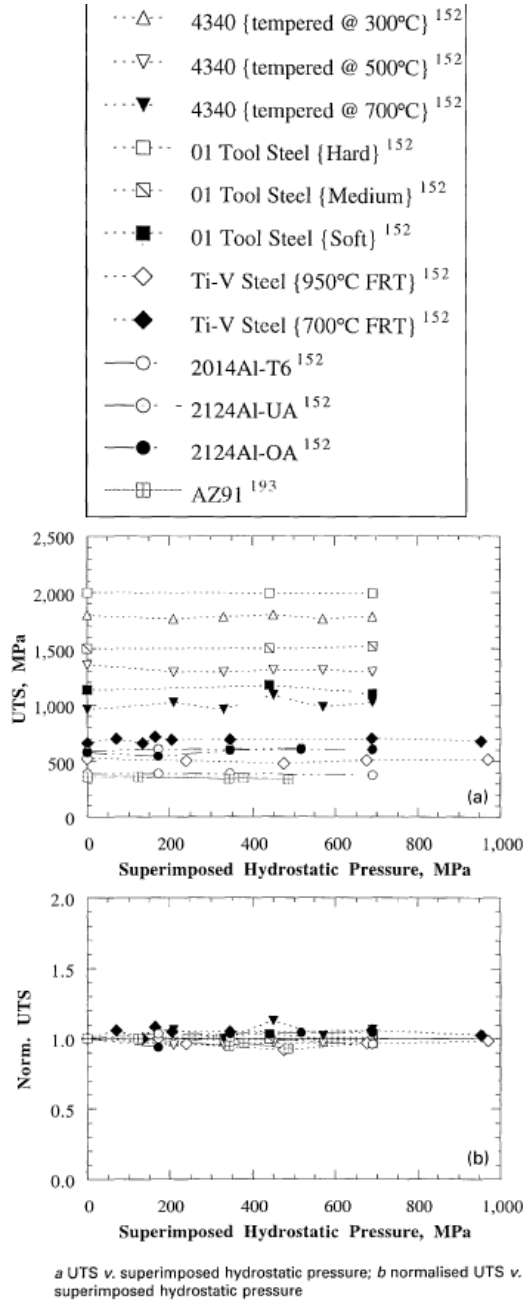

a UTS *v.* superimposed hydrostatic pressure; *b* normalised UTS *v.* superimposed hydrostatic pressure

14 Effect of pressure on UTS of various metals

J.J. Lewandowski and P. Lowhaphandu, International Materials Reviews, Vol.43, No.4, 1998.

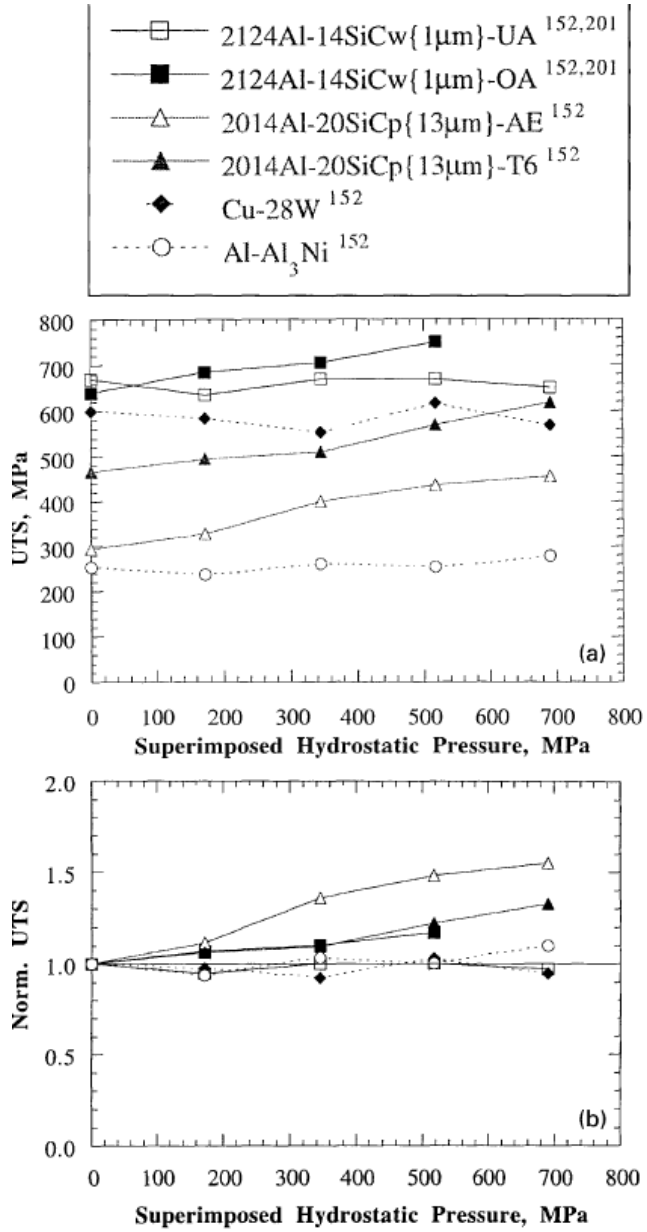

a UTS *v.* superimposed hydrostatic pressure; *b* normalised UTS *v.* superimposed hydrostatic pressure

15 Effect of pressure on UTS of discontinuously reinforced metal matrix composites

J.J. Lewandowski and P. Lowhaphandu, International Materials Reviews, Vol.43, No.4, 1998.

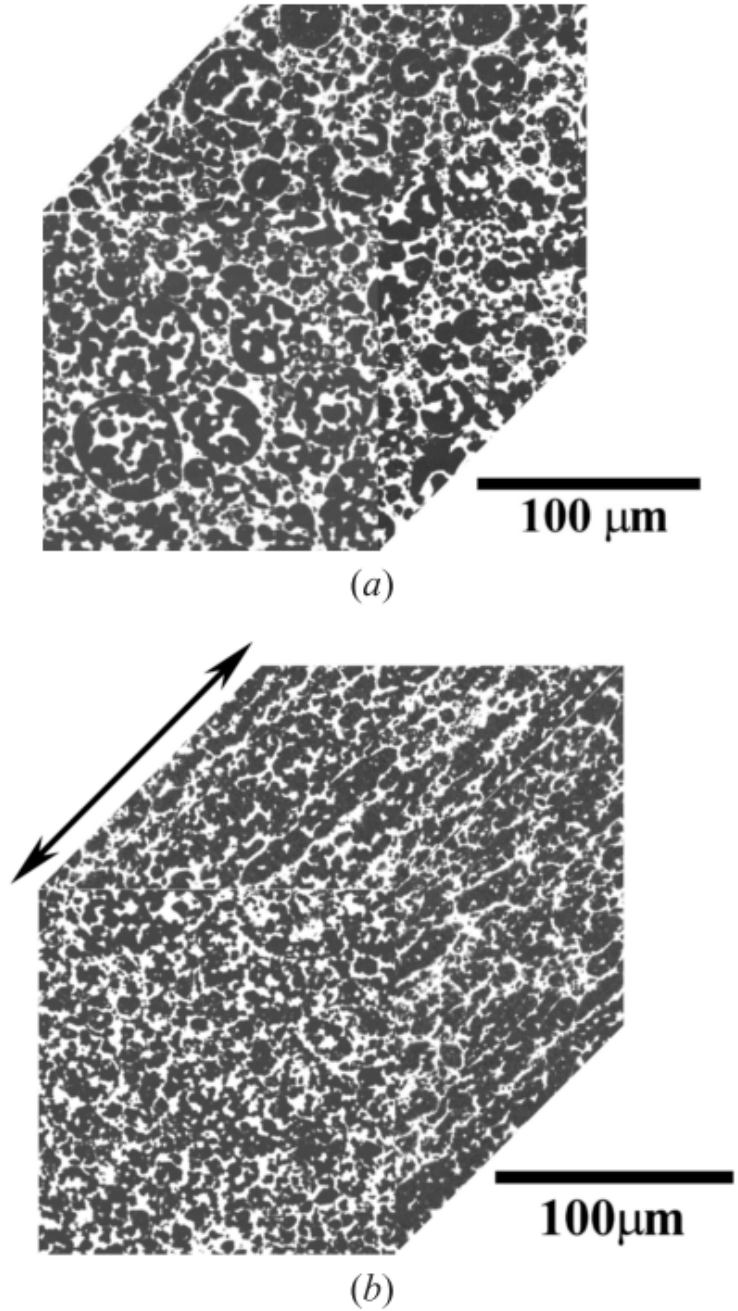

Fig. 3—Typical microstructure of (*a*) H material and (*b*) E material (extrusion direction indicated by arrow).

J. Larose and J.J. Lewandowski, Metall. Mater. Trans. A **33**, 3555 (2002).

IMS Institute for Materials Science Los Alamos

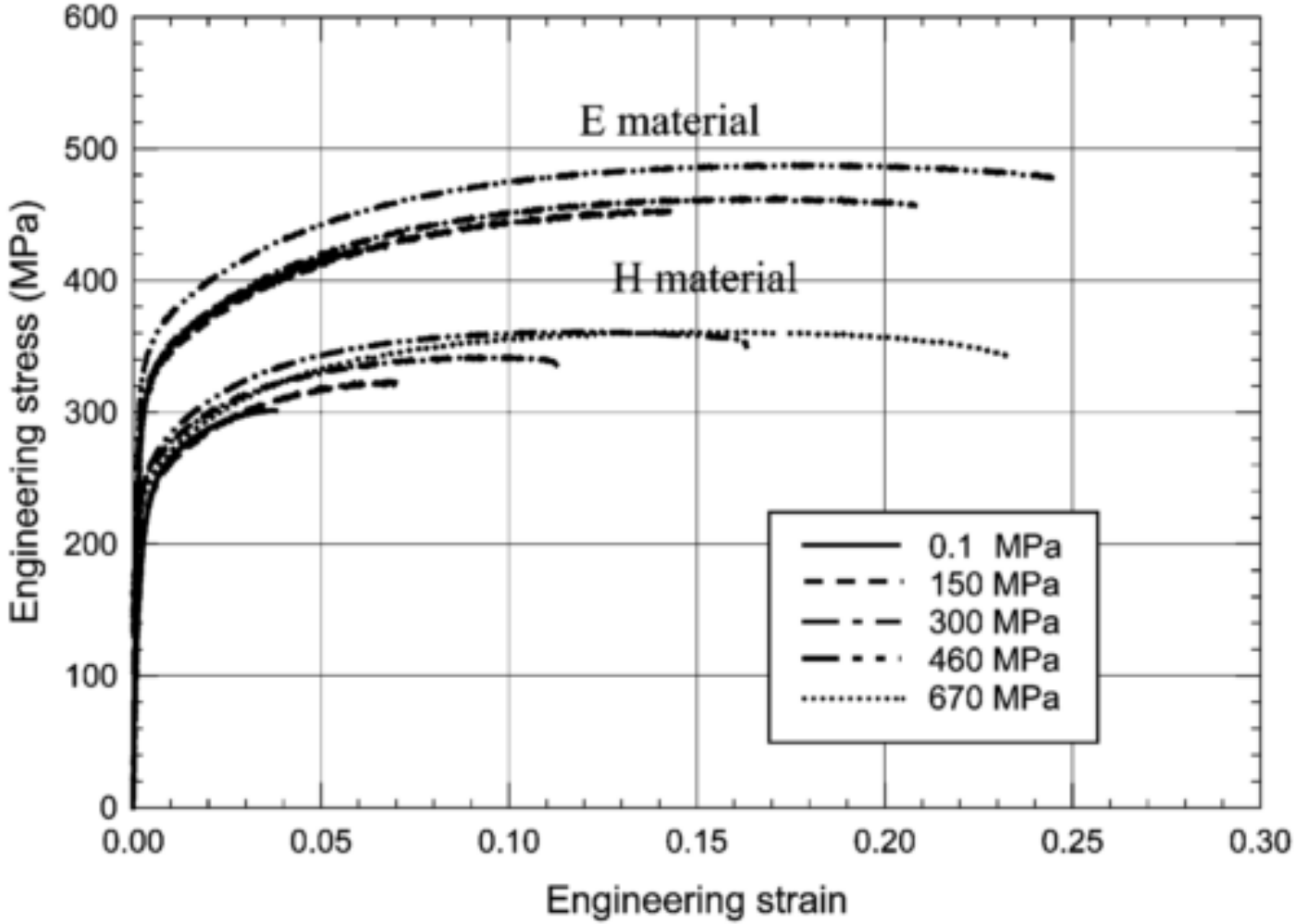

Fig. 4—Superimposed pressure effects on flow and fracture behavior of H and E materials.

IMS Institute for Materials Science Los Alamos

J. Larose and J.J. Lewandowski, Metall. Mater. Trans. A **33**, 3555 (2002).

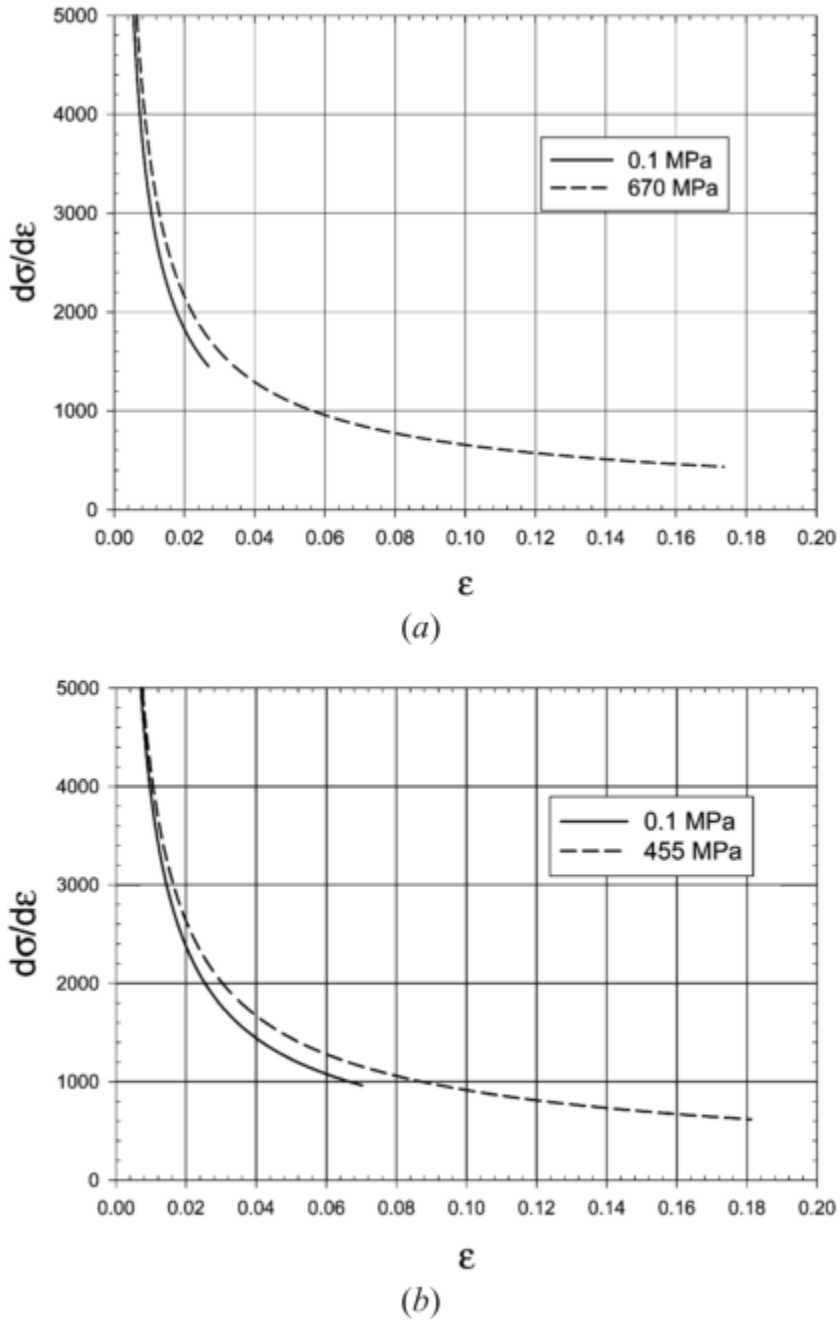

Fig. 10—Effects of confining pressure on $d\sigma/d\varepsilon$ *vs* ε in (*a*) H material and (*b*) E material.

J. Larose and J.J. Lewandowski, Metall. Mater. Trans. A **33**, 3555 (2002).

IMS Institute for Materials Science Los Alamos

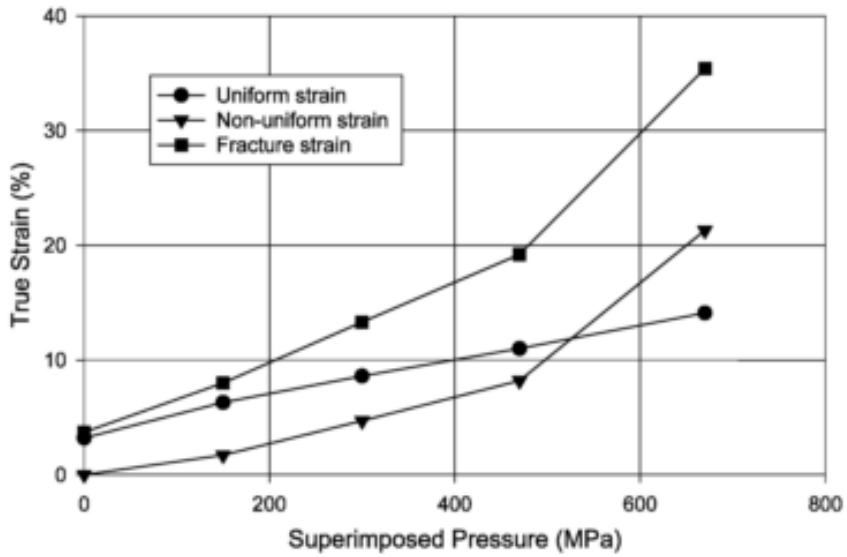

(*a*)

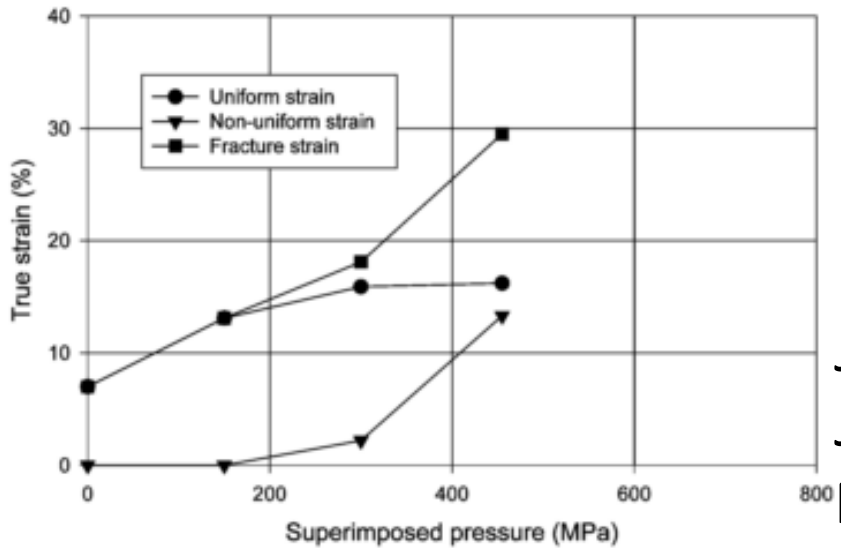

(*b*)

Fig. 11—Changes in uniform strain, nonuniform strain, and fracture strain with superimposed pressure for (*a*) H and (*b*) E materials.

J. Larose and J.J. Lewandowski, Metall. Mater. Trans.A **33**, 3555 (2002).

IMS Institute for Materials Science Los Alamos

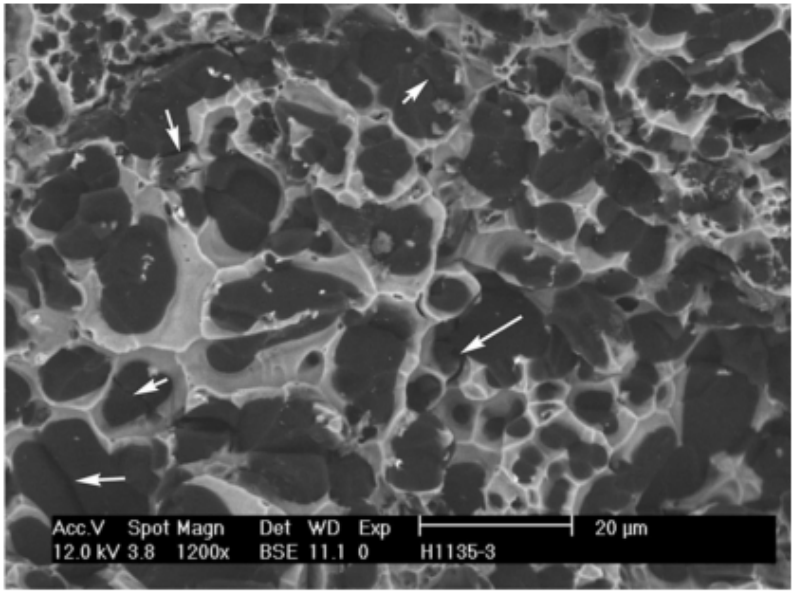

(*a*)

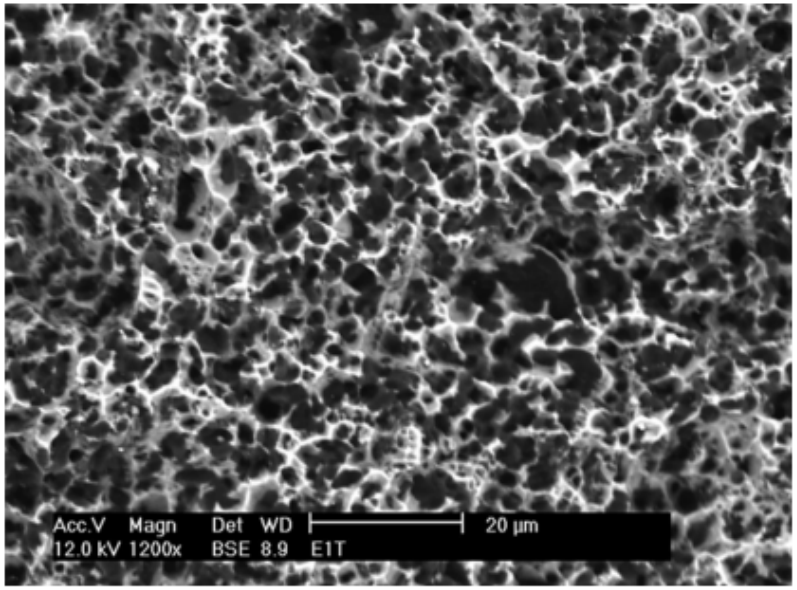

(*b*)

Fig. 6—Backscattered electron SEM views of the fracture surface of (*a*) H material and (*b*) E material Beryllium is dark phase. Secondary cracks in Be marked with arrows. Ductile rupture of Al is evident.

J. Larose and J.J. Lewandowski, Metall. Mater. Trans. A **33**, 3555 (2002).

IMS Institute for Materials Science Los Alamos

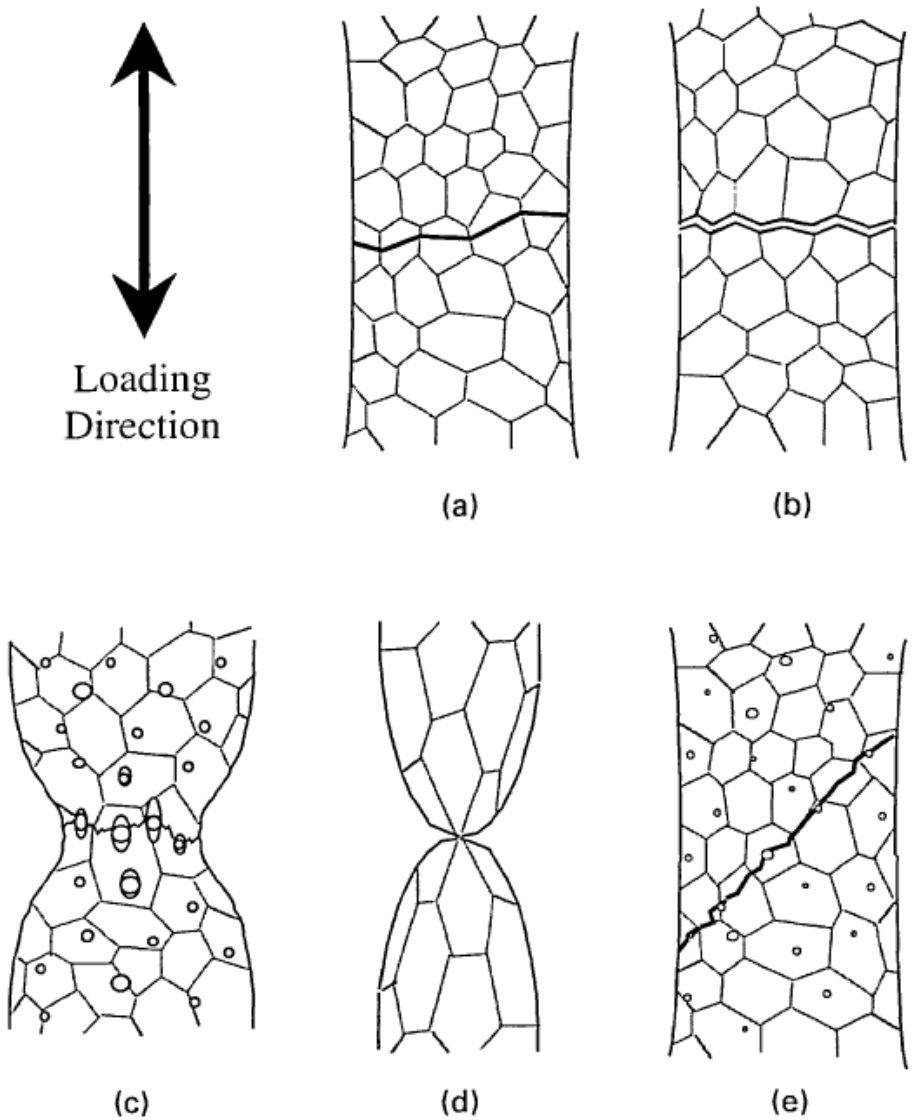

a transgranular cleavage; *b* intergranular fracture; *c* microvoid coalescence or dimpled rupture; *d* ductile rupture; *e* localised shear

16 General categories of fracture processes in metallic materials[351,352]

J.J. Lewandowski and P. Lowhaphandu, International Materials Reviews, Vol.43, No.4, 1998.

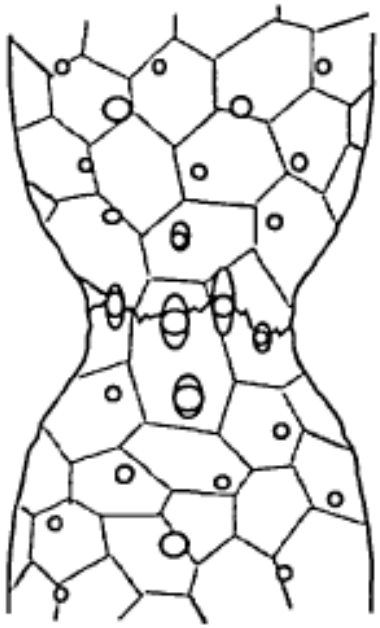

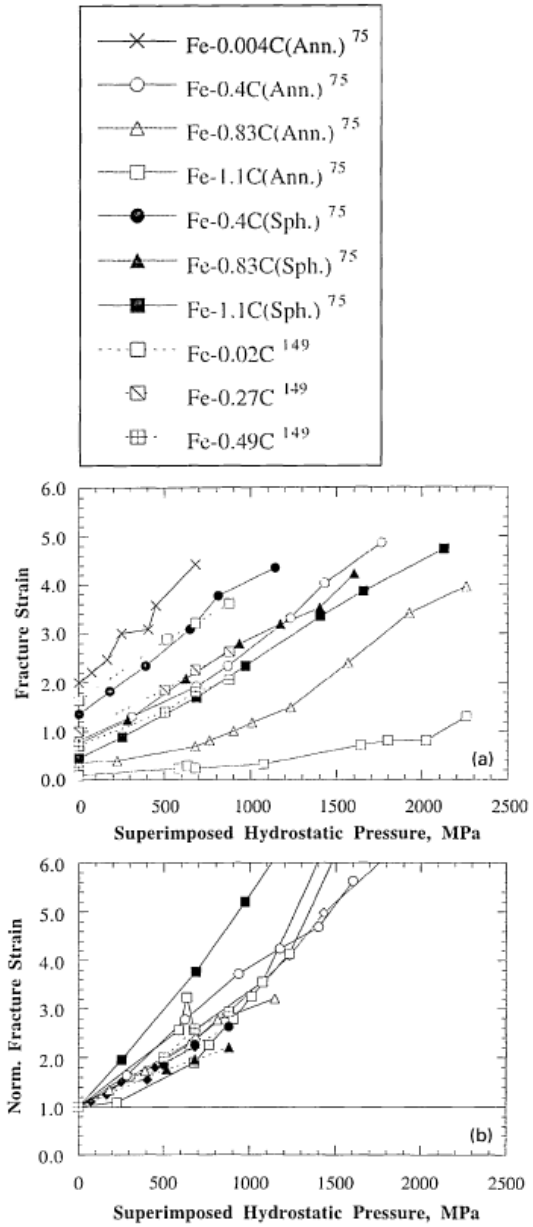

a fracture strain *v.* superimposed hydrostatic pressure; *b* normalised fracture strain *v.* superimposed hydrostatic pressure

23 Effect of pressure on fracture strain of Fe–C alloys

IMS Institute for Materials Science Los Alamos

J.J. Lewandowski and P. Lowhaphandu, International Materials Reviews, Vol.43, No.4, 1998.

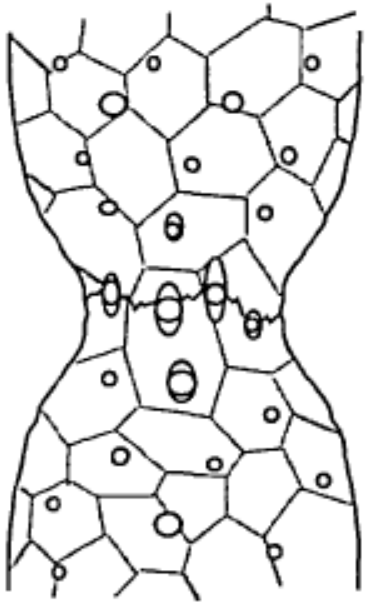

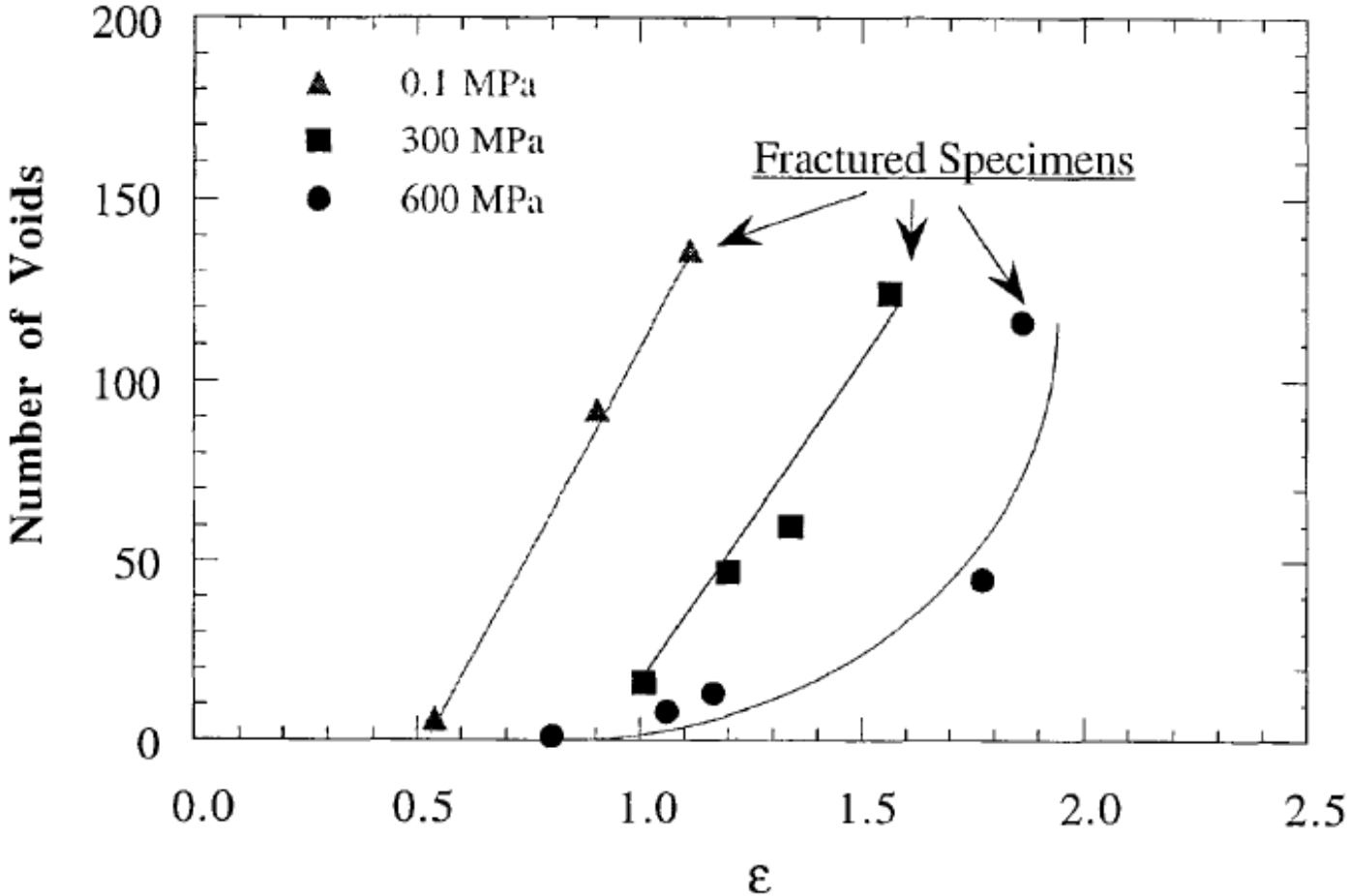

25 Number of voids in centre of necked tension specimen tested at various levels of superimposed hydrostatic pressure to the indicated levels of strain ε for spheroidised 0·5%C steel (after Ref. 87)

IMS Institute for Materials Science Los Alamos

J.J. Lewandowski and P. Lowhaphandu, International Materials Reviews, Vol.43, No.4, 1998.

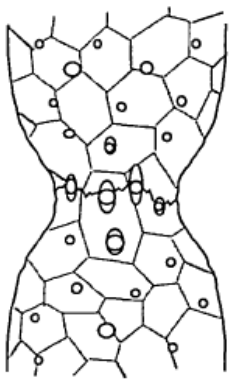

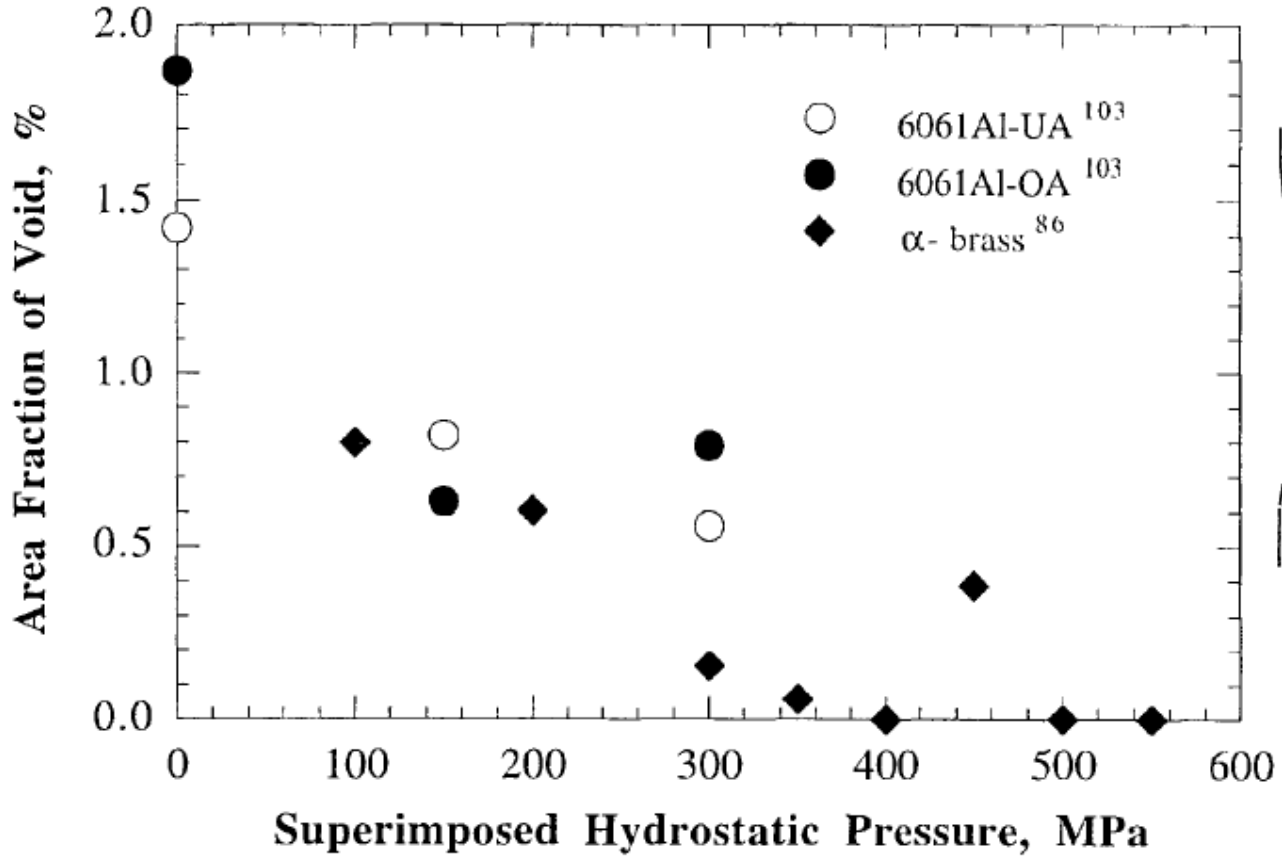

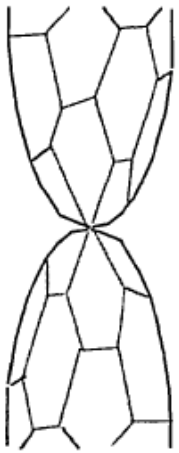

29 Area fraction of voids in 6061Al–UA/OA (Ref. 103) and α-brass[86] as function of superimposed hydrostatic pressure

J.J. Lewandowski and P. Lowhaphandu, International Materials Reviews, Vol.43, No.4, 1998.

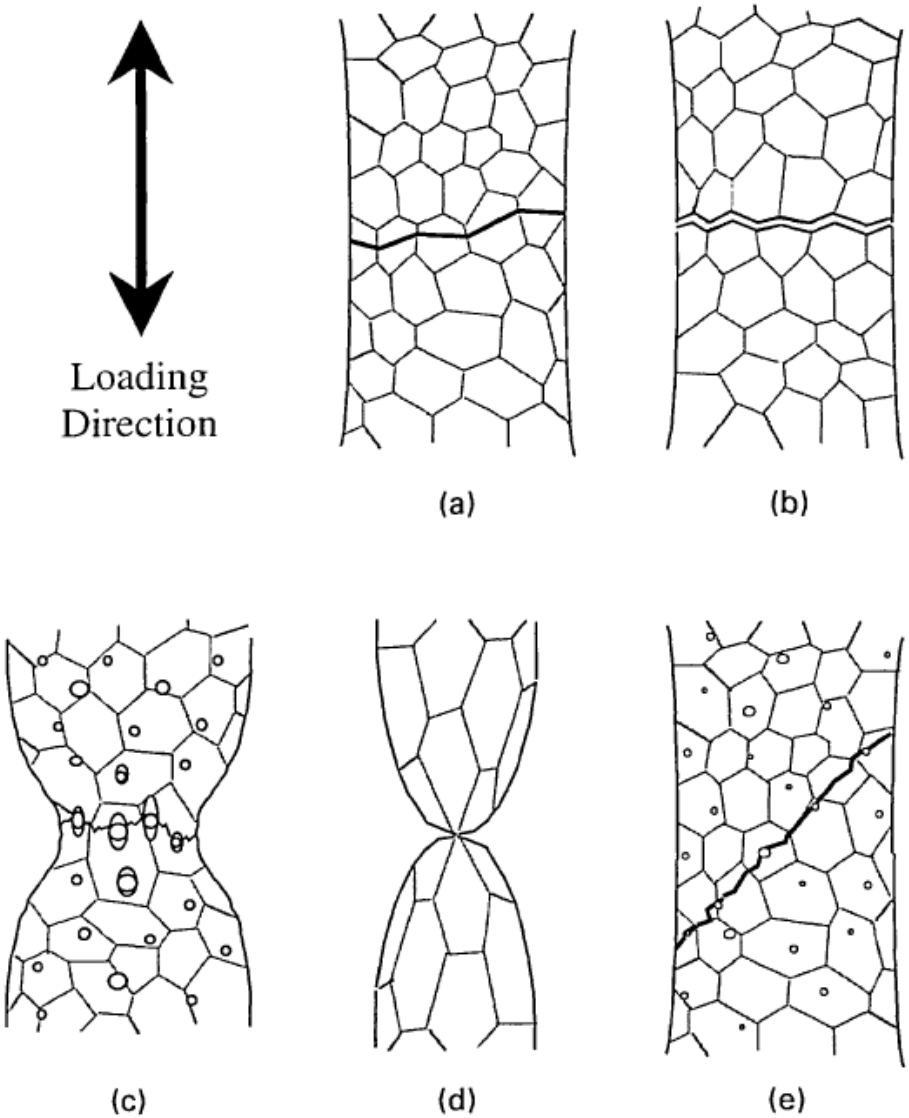

a transgranular cleavage; *b* intergranular fracture; *c* microvoid coalescence or dimpled rupture; *d* ductile rupture; *e* localised shear

16 General categories of fracture processes in metallic materials[351,352]

J.J. Lewandowski and P. Lowhaphandu, International Materials Reviews, Vol.43, No.4, 1998.

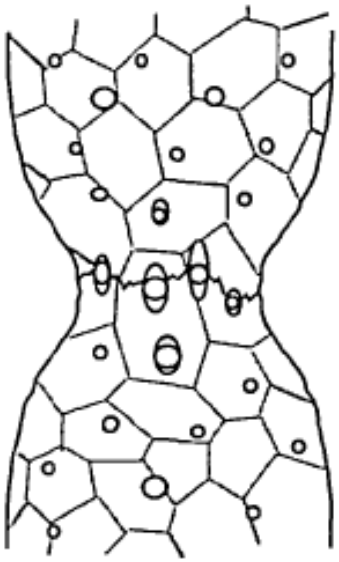

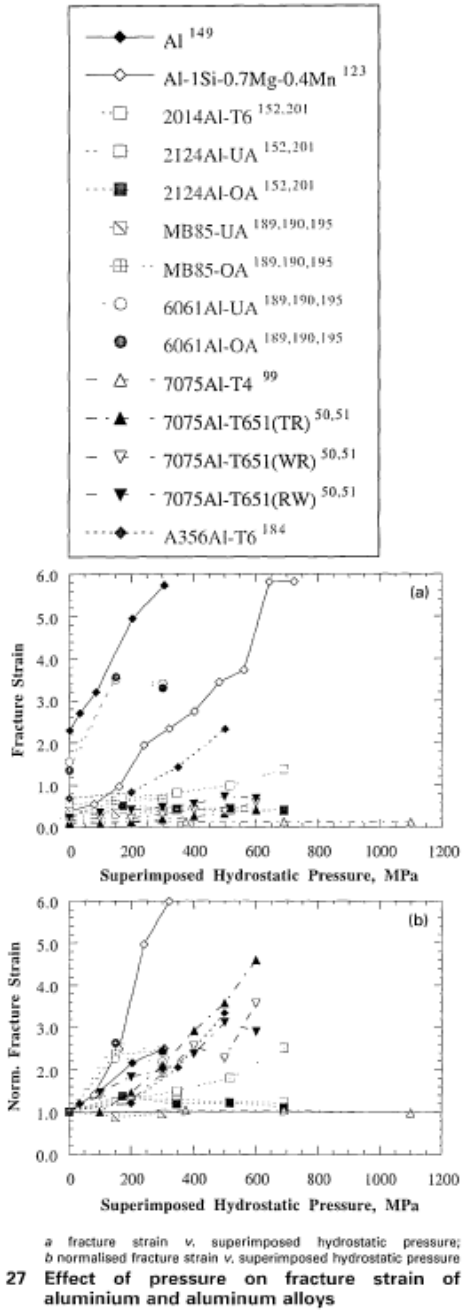

a fracture strain *v.* superimposed hydrostatic pressure; *b* normalised fracture strain *v.* superimposed hydrostatic pressure

27 Effect of pressure on fracture strain of aluminium and aluminum alloys

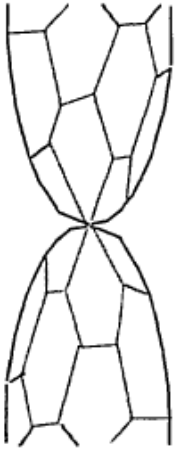

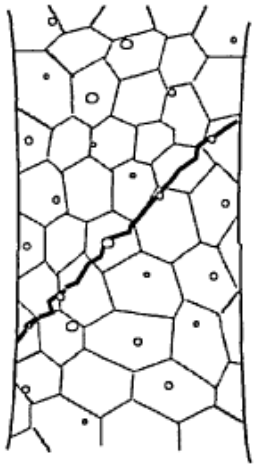

IMS Institute for Materials Science Los Alamos

J.J. Lewandowski and P. Lowhaphandu, International Materials Reviews, Vol.43, No.4, 1998.

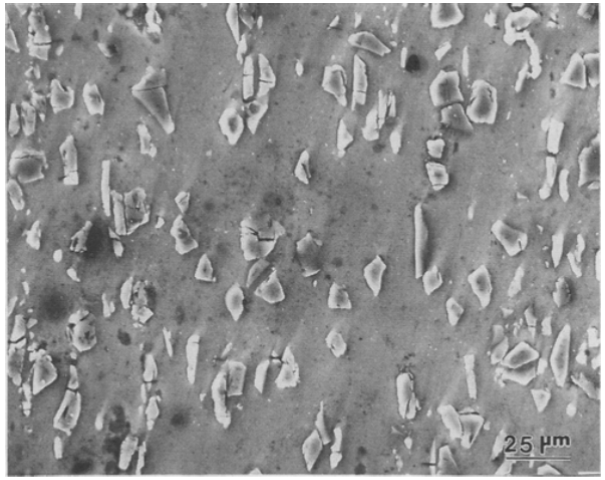

Fig. 11 — Micrograph showing cracked SiC_p on the surface of the 13 μm-UA specimen after about 6.3 pct global plastic strain, ε_{gpl}.

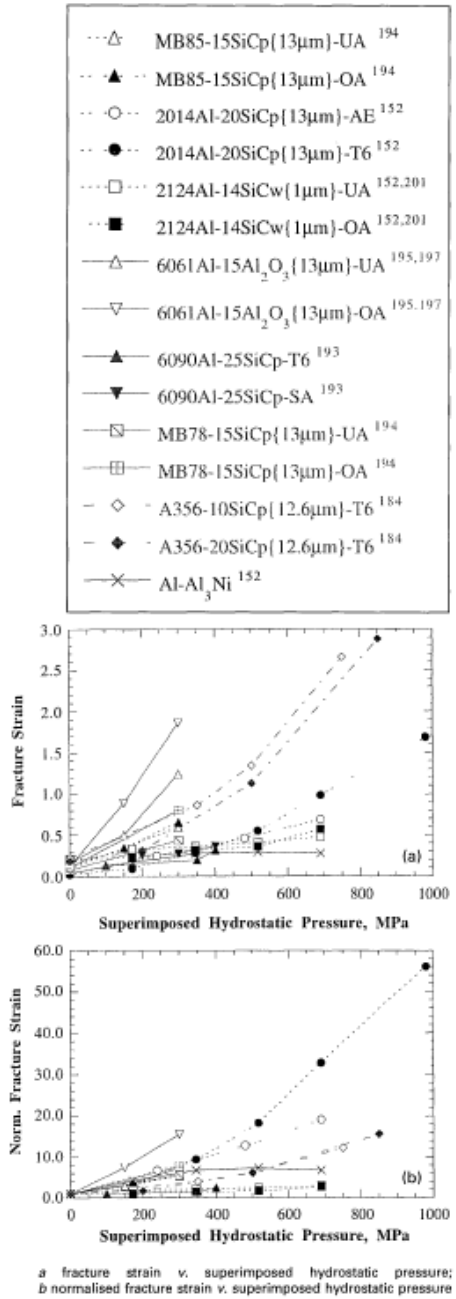

a fracture strain *v.* superimposed hydrostatic pressure; *b* normalised fracture strain *v.* superimposed hydrostatic pressure

31 Effect of pressure on fracture strain of discontinuously reinforced aluminium matrix composites

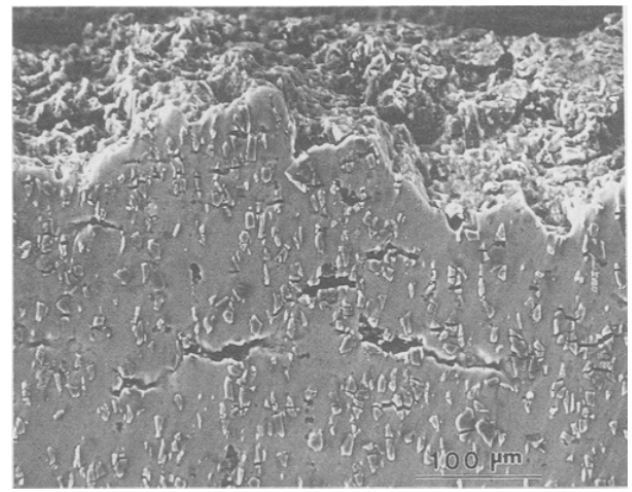

Fig. 16 — Micrograph showing area near fracture surface for the 13 μm-UA specimen. Fracture surface is located at top.

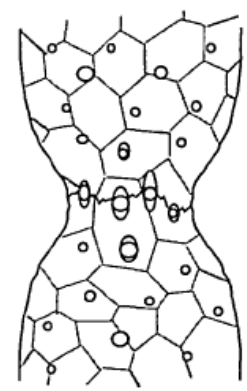

IMS Institute for Materials Science Los Alamos

J.J. Lewandowski and P. Lowhaphandu, International Materials Reviews, Vol.43, No.4, 1998.

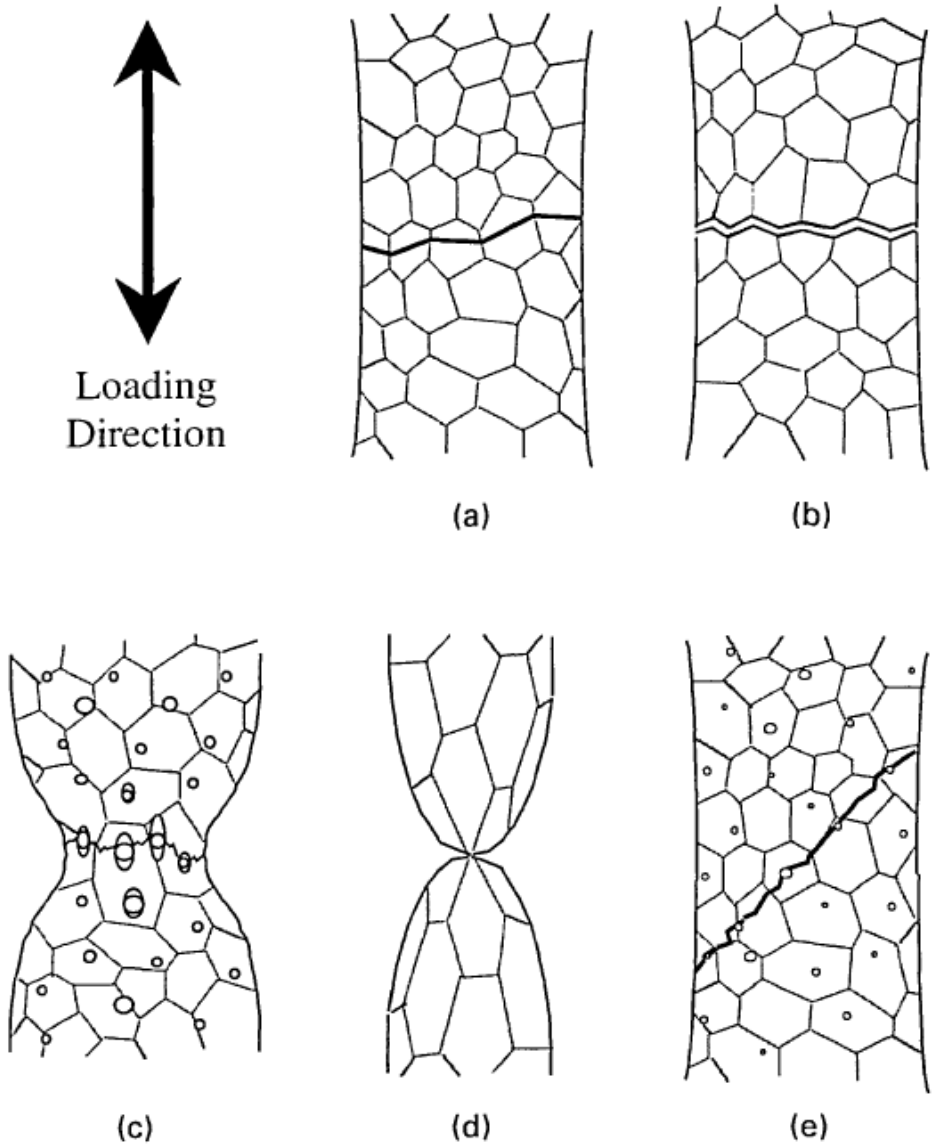

a transgranular cleavage; *b* intergranular fracture; *c* microvoid coalescence or dimpled rupture; *d* ductile rupture; *e* localised shear

16 General categories of fracture processes in metallic materials[351,352]

J.J. Lewandowski and P. Lowhaphandu, International Materials Reviews, Vol.43, No.4, 1998.

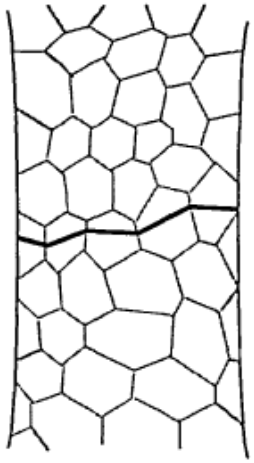

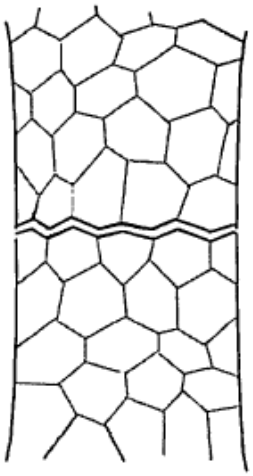

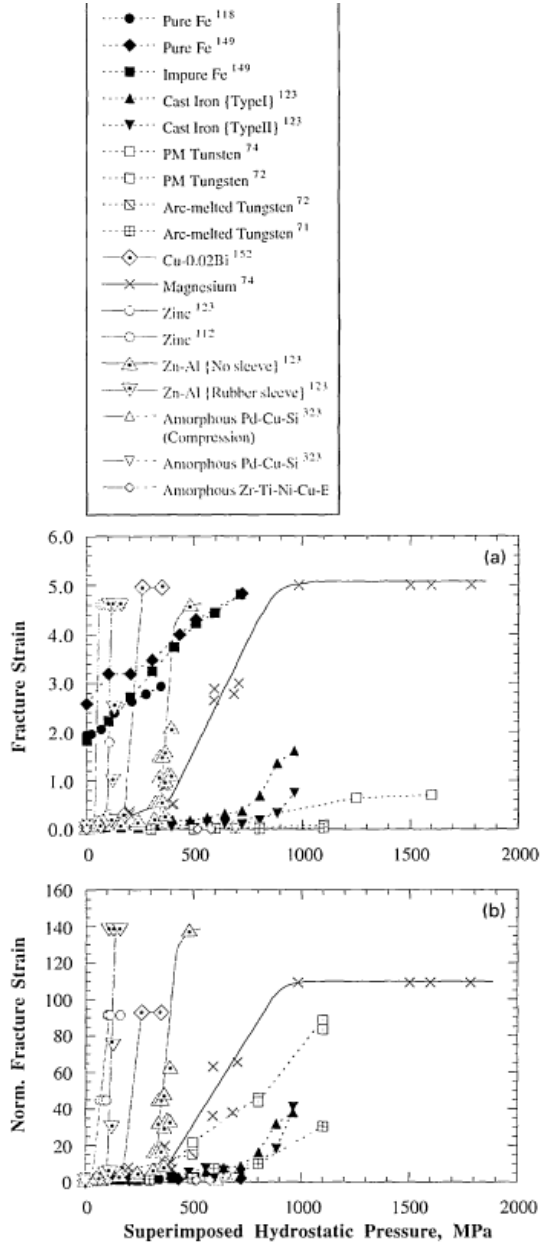

a fracture strain *v.* superimposed hydrostatic pressure; *b* normalised fracture strain *v.* superimposed hydrostatic pressure

26 Effect of pressure on fracture strain of some bcc metals, amorphous metals, and other brittle metals

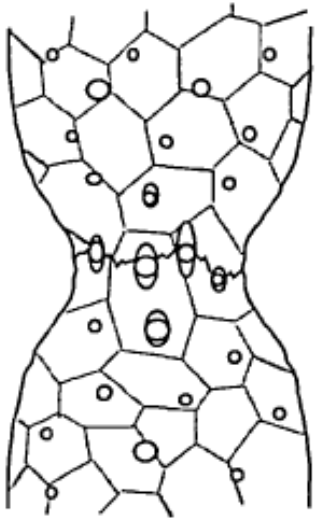

IMS Institute for Materials Science Los Alamos

J.J. Lewandowski and P. Lowhaphandu, International Materials Reviews, Vol.43, No.4, 1998.

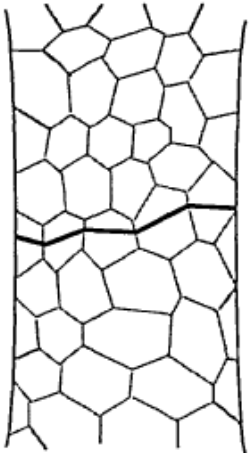

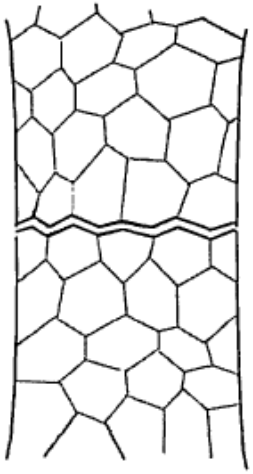

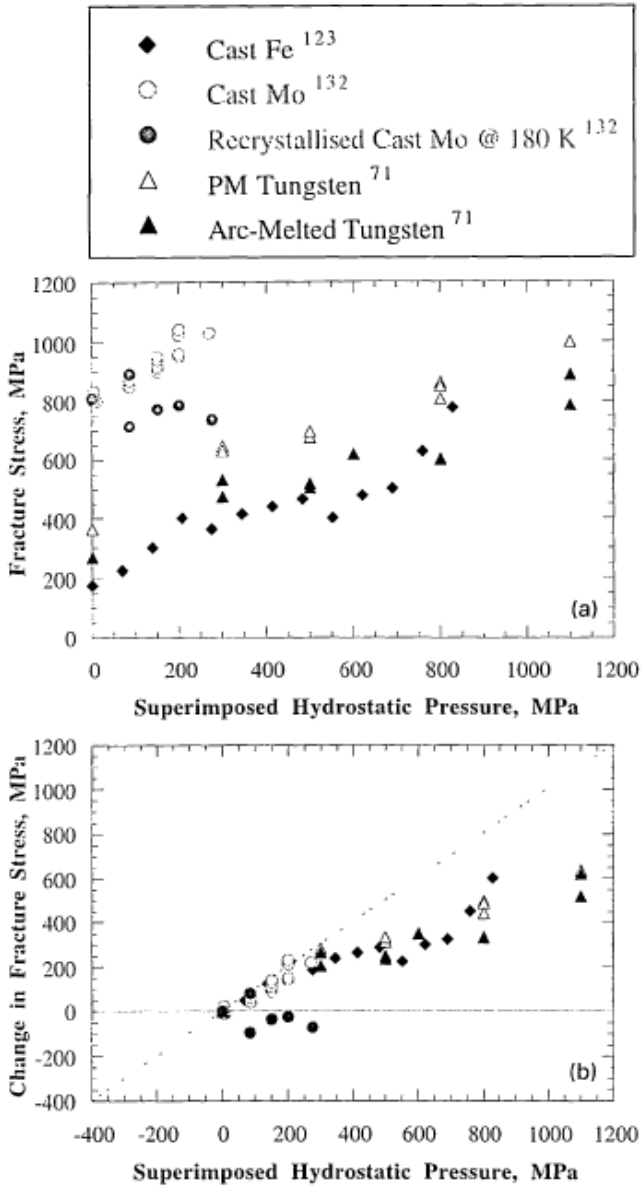

a fracture stress *v.* superimposed hydrostatic pressure; *b* normalised fracture stress *v.* superimposed hydrostatic pressure

38 Effect of pressure on fracture stress of bcc metals

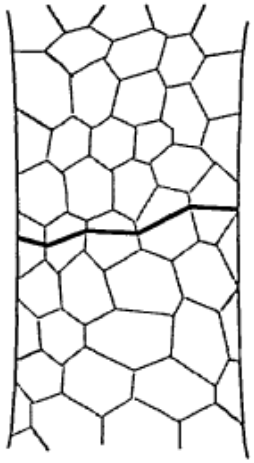

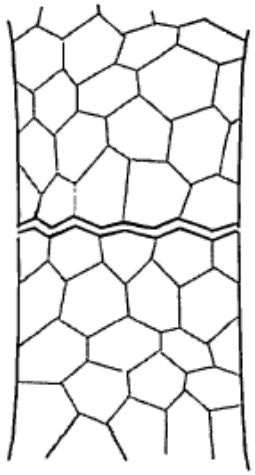

IMS Institute for Materials Science Los Alamos

J.J. Lewandowski and P. Lowhaphandu, International Materials Reviews, Vol.43, No.4, 1998.

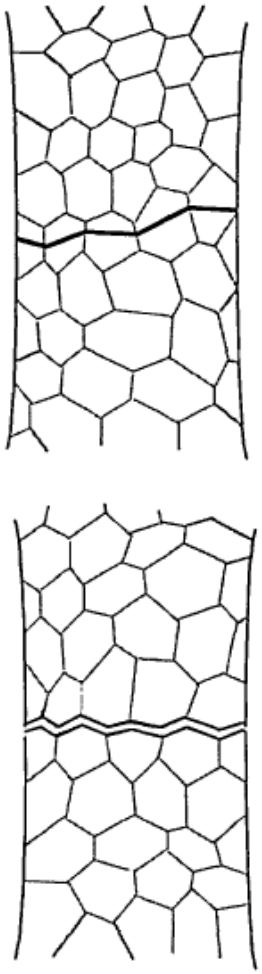

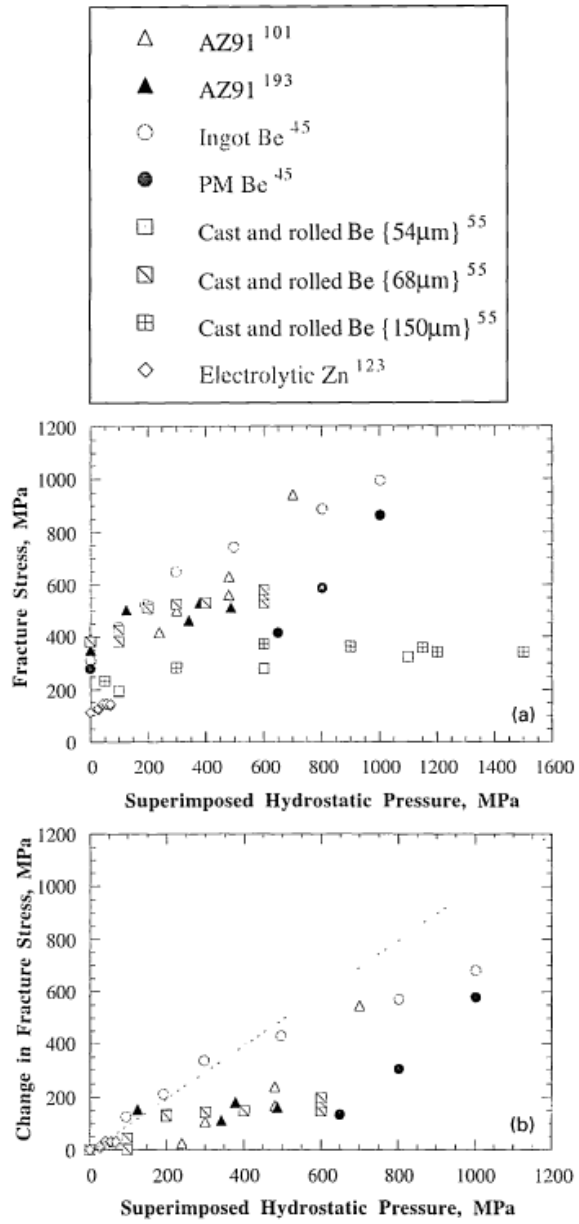

a fracture stress *v.* superimposed hydrostatic pressure; *b* normalised fracture stress *v.* superimposed hydrostatic pressure

39 Effect of pressure on fracture stress of hcp metals

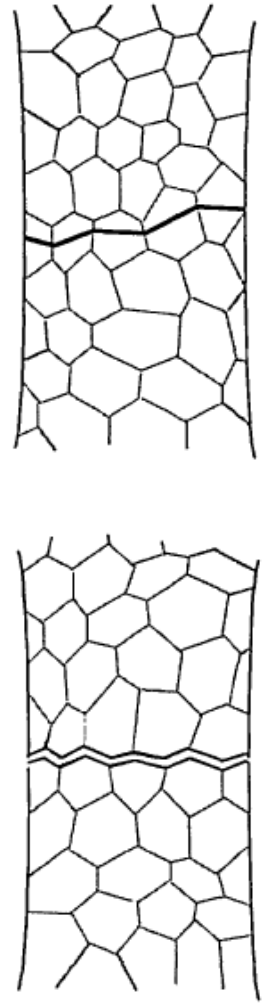

IMS Institute for Materials Science Los Alamos

J.J. Lewandowski and P. Lowhaphandu, International Materials Reviews, Vol.43, No.4, 1998.

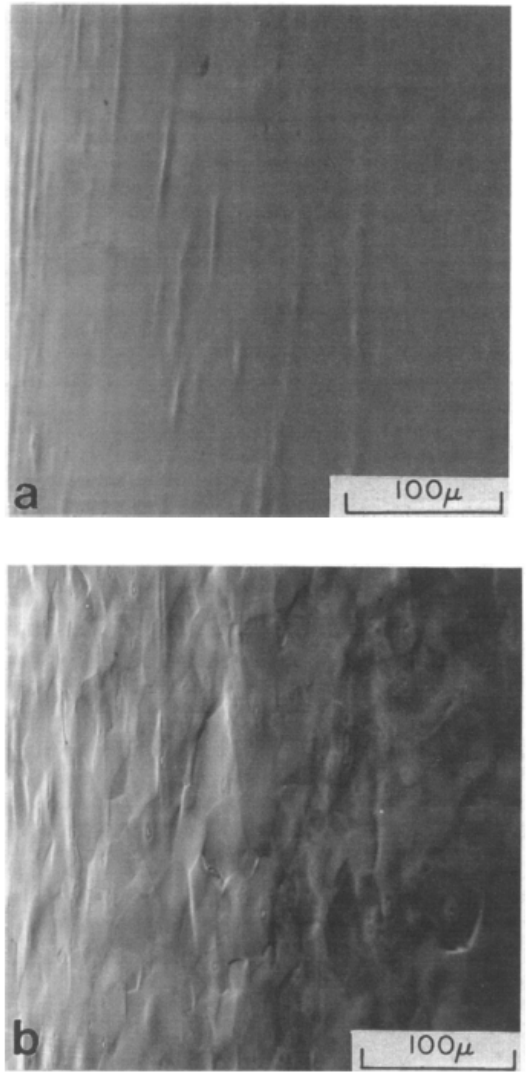

Fig. 6—Low-magnification SEM micrographs of gage lengths of samples strained in tension at (*a*) 0.1 MPa and (*b*) 500 MPa. Loading axis is vertical.

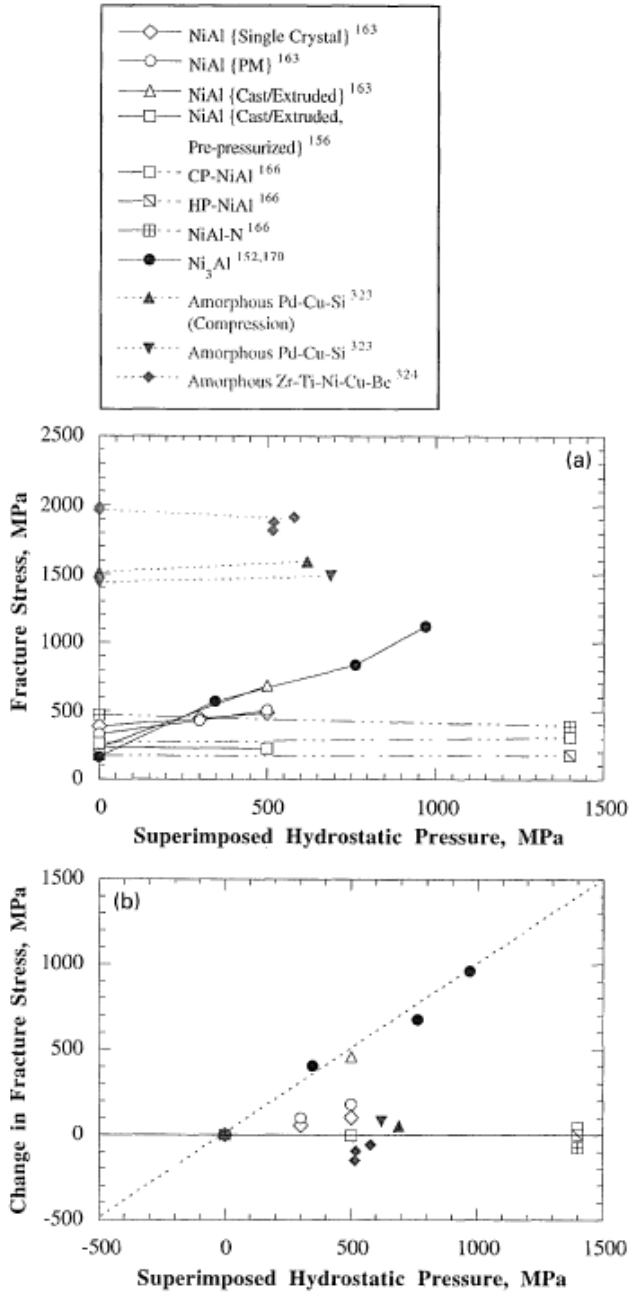

a fracture stress *v.* superimposed hydrostatic pressure; *b* normalised fracture stress *v.* superimposed hydrostatic pressure

40 Effect of pressure on fracture stress of NiAl, Ni_3Al, and amorphous metals

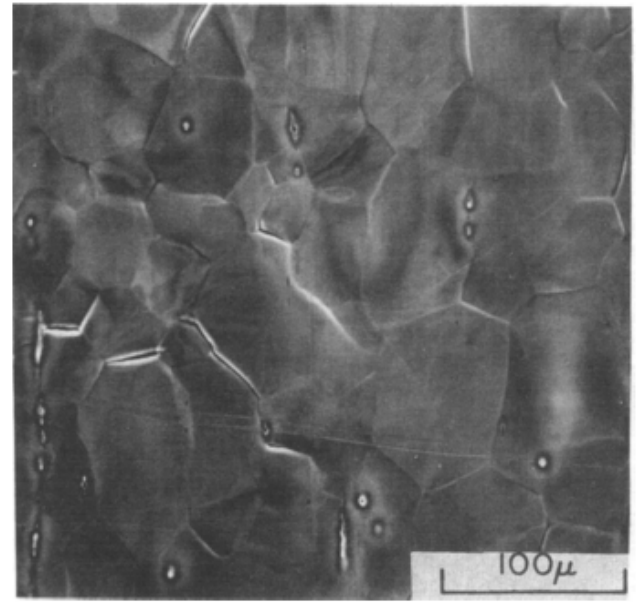

Fig. 8—SEM micrograph of microcracks on the external surface of the sample tested in tension at 500 MPa to 10 pct strain. Loading axis is vertical, and note that only IG microcracks are visible.

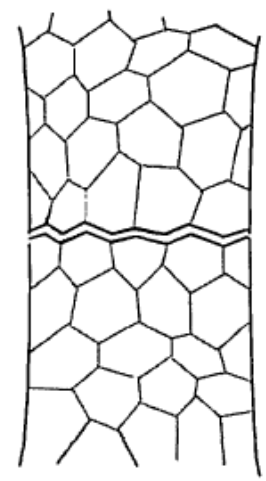

R.W. Margevicius and J.J. Lewandowski, Metall. Mat. Trans. A **25**, 1457 (1994).

IMS Institute for Materials Science Los Alamos

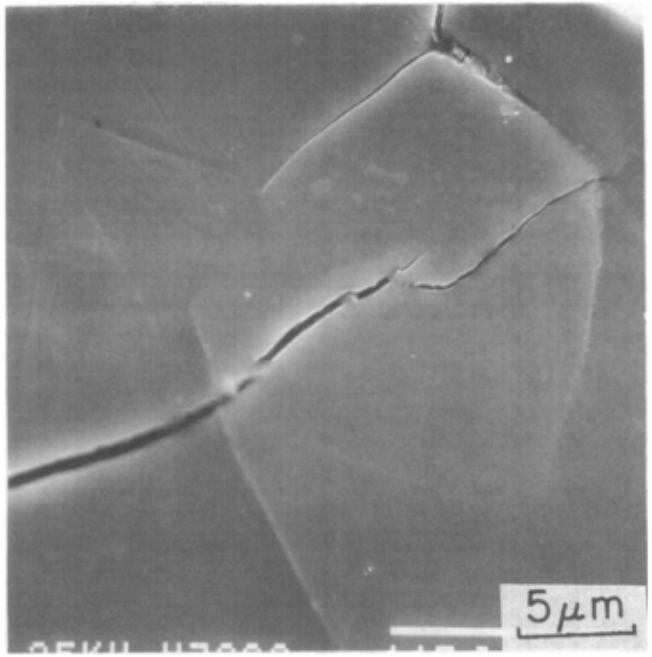

Fig. 9—SEM micrograph of TG microcrack on the external surface of the sample tested in tension at 500 MPa to 10 pct strain. Loading axis is vertical.

R.W. Margevicius and J.J. Lewandowski, Metall. Mat. Trans. A **25**, 1457 (1994).

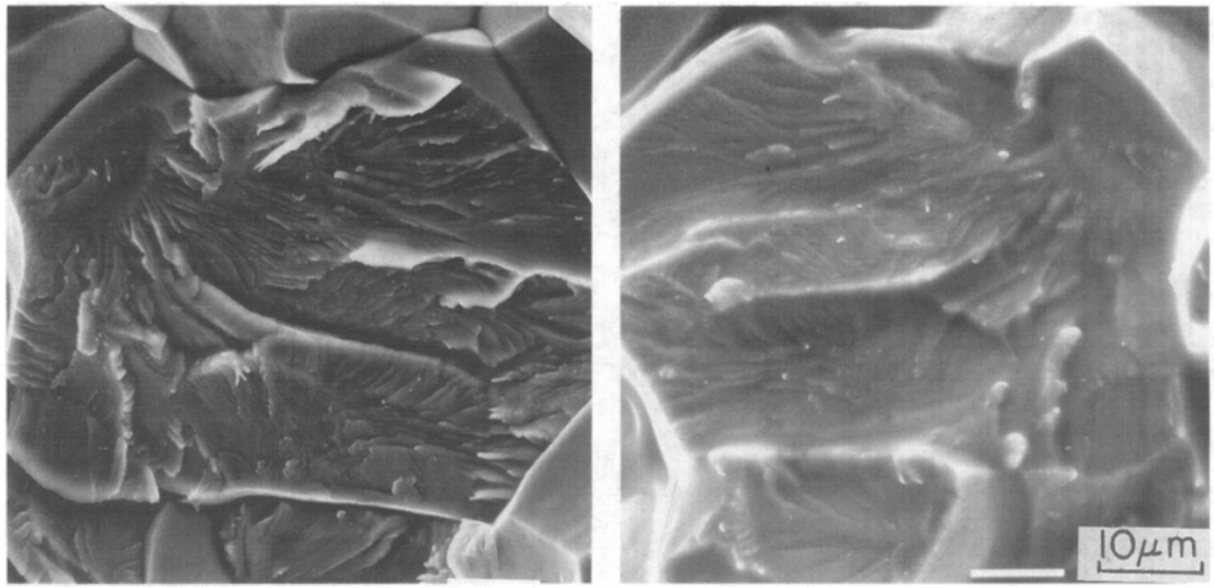

Fig. 14—SEM micrographs of matching fracture surfaces of the cast NiAl specimens tested at 500 MPa, showing ridge-to-ridge matching of the TG portions of the fracture surface.

IMS
Institute for Materials Science
Los Alamos

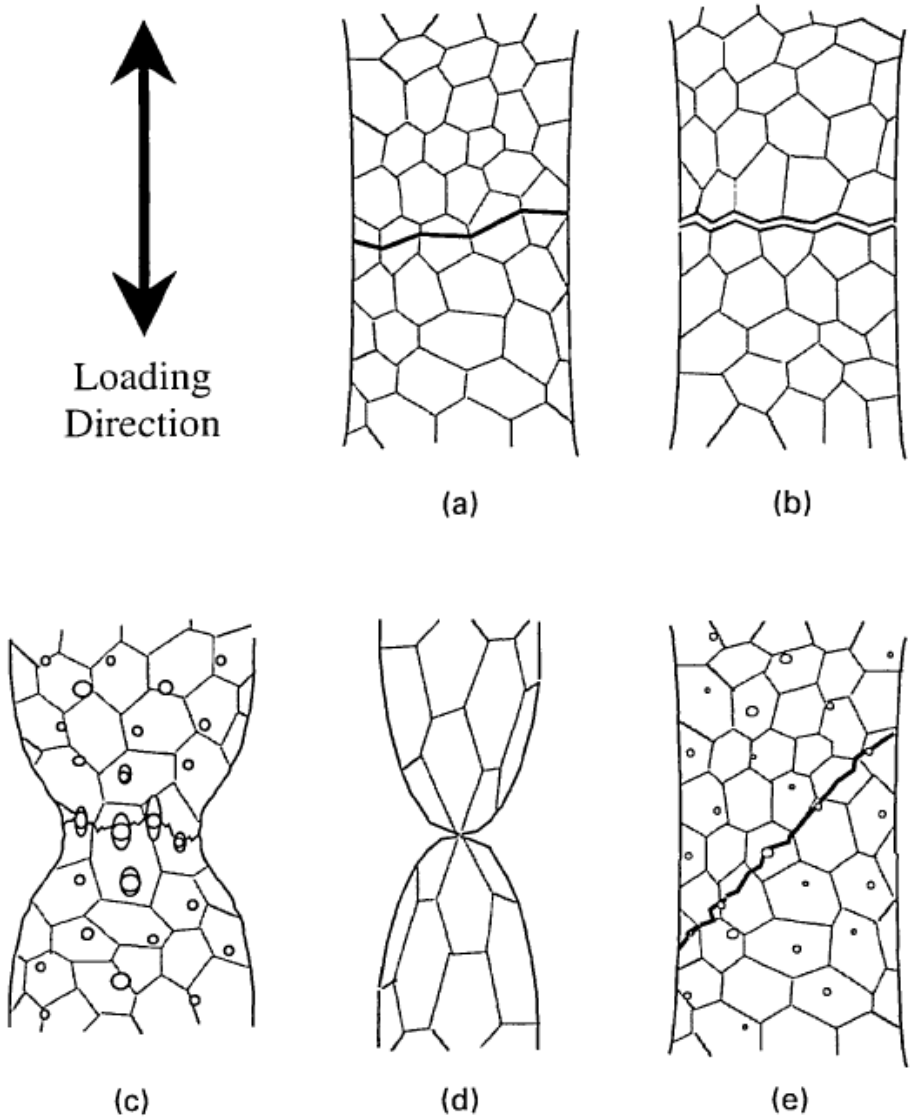

a transgranular cleavage; *b* intergranular fracture; *c* microvoid coalescence or dimpled rupture; *d* ductile rupture; *e* localised shear

16 General categories of fracture processes in metallic materials[351,352]

J.J. Lewandowski and P. Lowhaphandu, International Materials Reviews, Vol.43, No.4, 1998.

Summary

High Pressure Effects on Metals and Metallic Composites

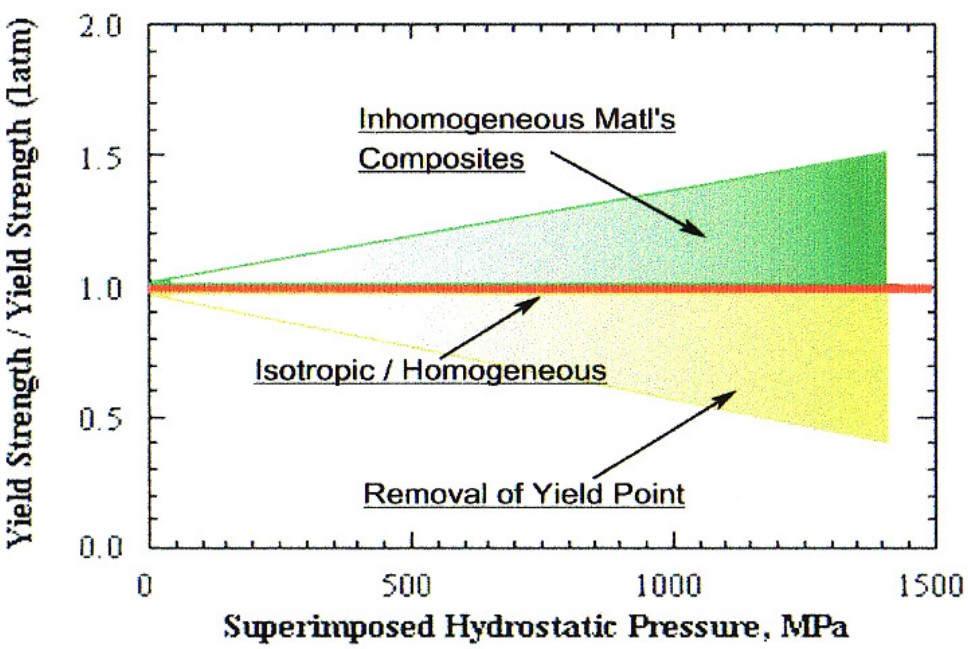

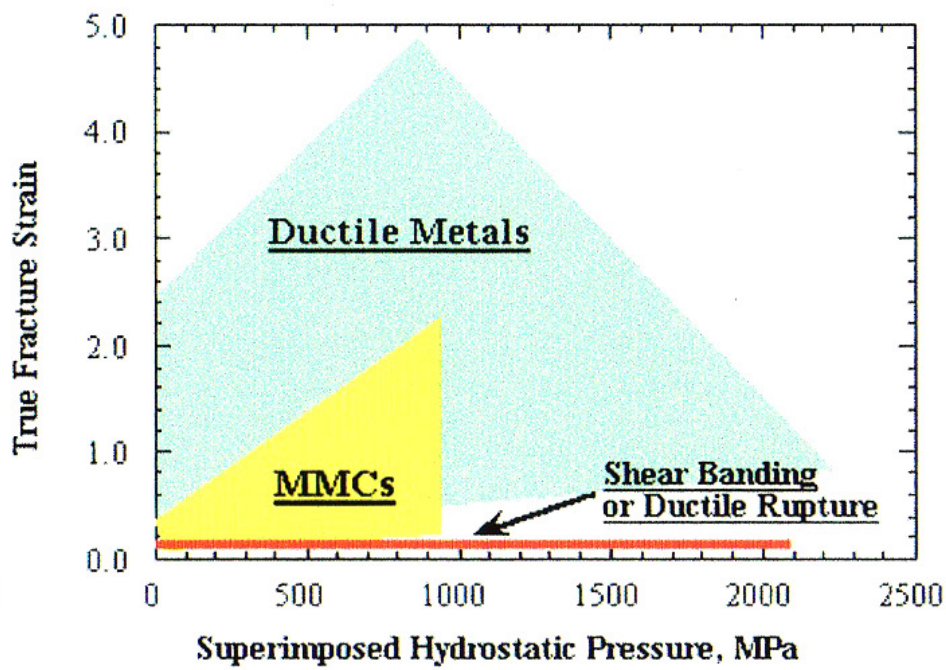

Outline

- High Pressure Testing Rigs
  - Pressure Media: Gas, Oil
  - Internal Load Cell, Pressure Measurement
- Pressure Effects on Flow of Metallic Alloys
  - Yielding
    - Cubic Systems
    - Non-Cubic Systems
    - Particle-containing systems
  - UTS

- Pressure Effects on Fracture of Metallic Alloys
    - Fracture Micro-mechanisms
    - Pressure Effects on Ductility/Fracture
- Pressure Effects on Composites, Intermetallics
  - Flow
    - Ductility/Fracture
    - Pressure and Temperature Effects
        - Implications on Deformation Processing
- Hydrostatic Extrusion
    - Concept
    - Examples (Composites, NiAl)
    - ODS Tubes?
        - Billet Design, Initial Results

IMS
Institute for Materials Science
Los Alamos

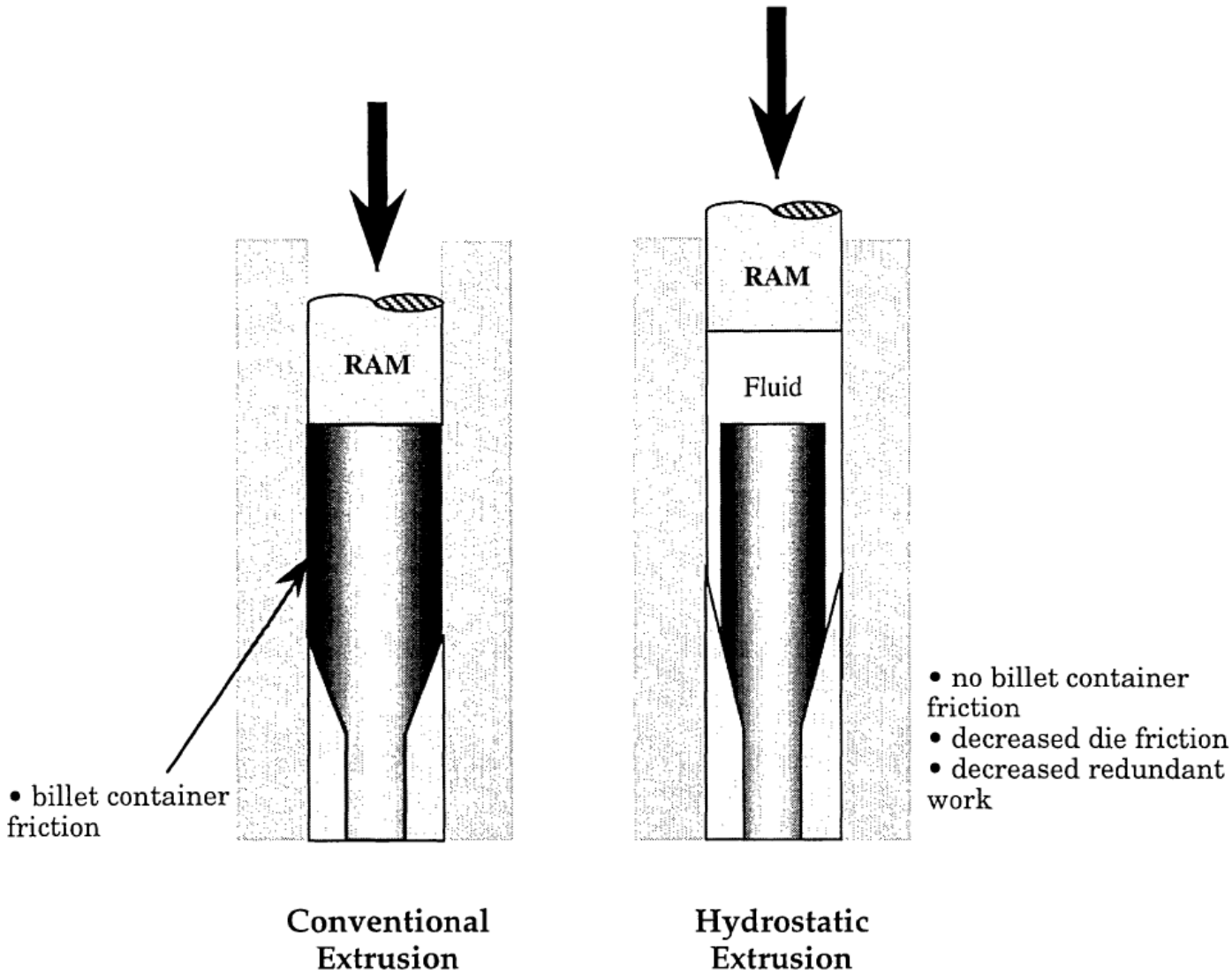

48 Comparison of apparatus for conventional extrusion and hydrostatic extrusion[186,187,398]

J.J. Lewandowski and P. Lowhaphandu, International Materials Reviews, Vol.43, No.4, 1998.

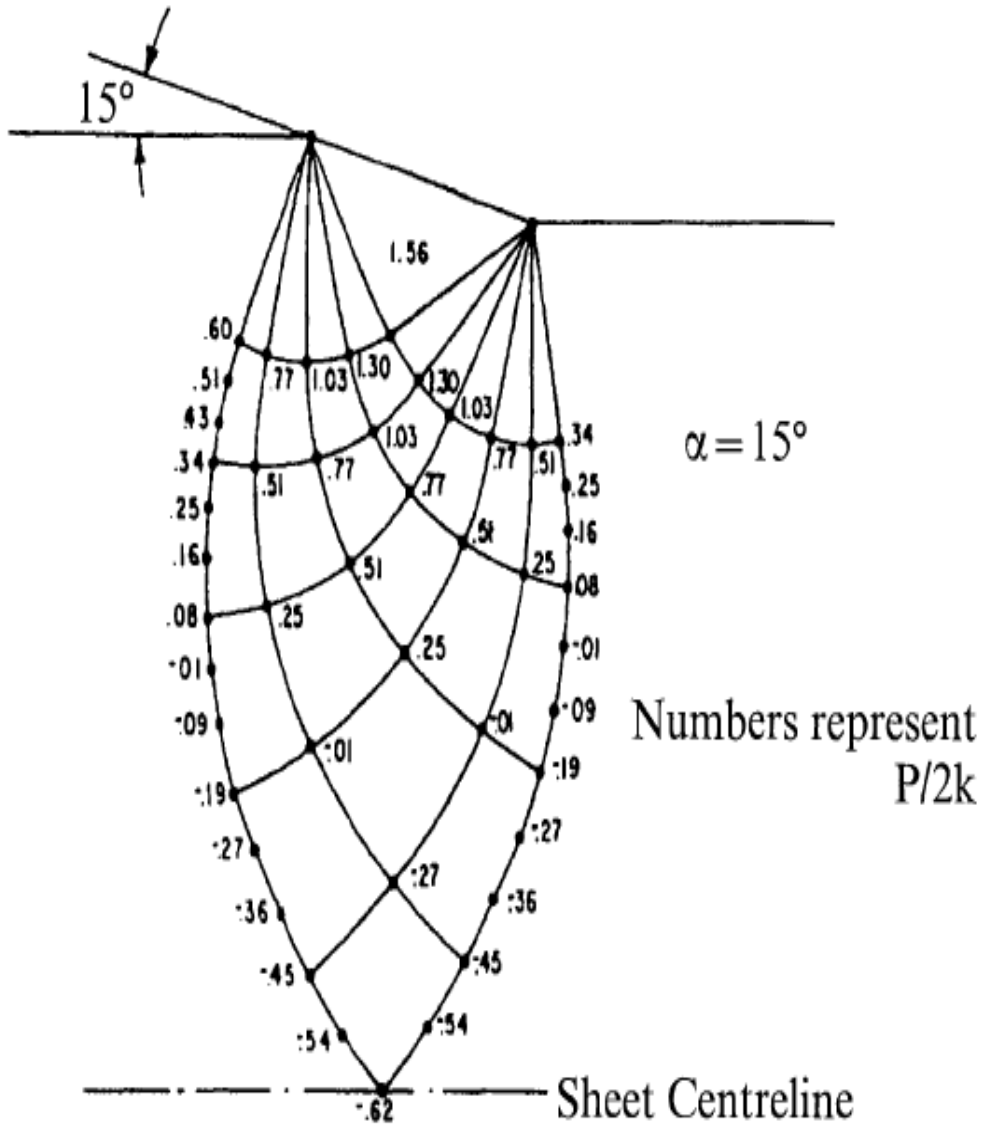

45 Variation in hydrostatic pressure in deformation zone for strip drawing based on field shown: note that negative values are tensile[414]

J.J. Lewandowski and P. Lowhaphandu, International Materials Reviews, Vol.43, No.4, 1998.

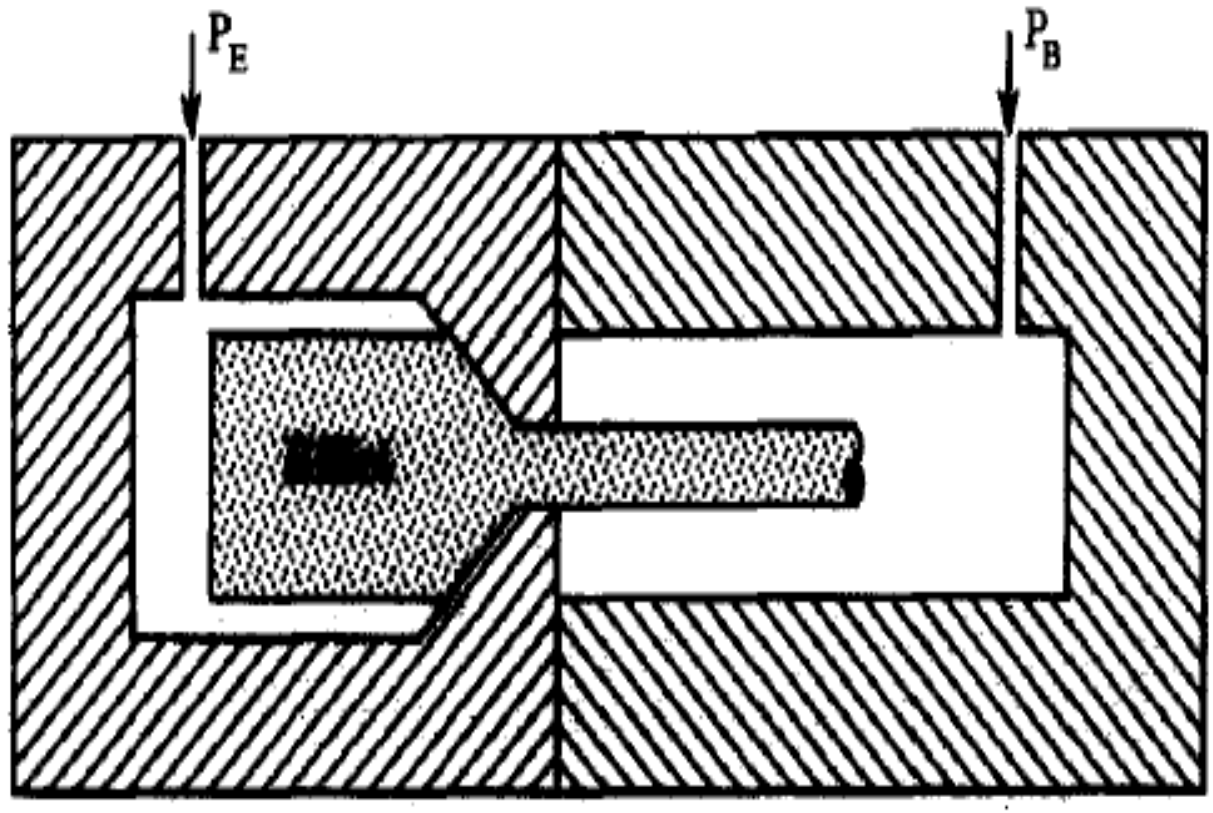

$$\text{Extrusion Pressure Ratio} = \frac{P_B}{P_E}$$

P_E = Extrusion Pressure
P_B = Back Pressure

Fig. 3. Schematic representation of the hydrostatic extrusion apparatus.

IMS Institute for Materials Science Los Alamos

J.J. Lewandowski and P. Lowhaphandu, International Materials Reviews, Vol.43, No.4, 1998.

Table 4 Summary of hydrostatic extrusion data for various materials without back pressure

Material	Die angle, deg	Hardness, HV Billet*	Hardness, HV Product†
Iron and steel			
Armco iron[304,305]	45	76	...
Armco Iron[304,305]	90	76	...
Mild steel[304,305]	45	113	195–277
Steel (0·15C)[290–292,295,308]	45	...	...
AISI 1020 steel[398]	20	110	285
AISI 1020 steel[307]	90	...	...
Zn 58[304,305]	45	135	250–320
Zn 8[304,305]	45	148	240–280
D-2 steel[304,305]	45	243	313
D-2 steel[304,305]	45	243	370
AISI 4340 steel[397]	45	195	285–301
AISI 4340 steel[397]	45	195	301–393
High speed steel[304,305]	45	260	390–420
Rex 448[304,305]	45	340	370
High tensile[304,305]	45	374	390–470
Cast iron[306]	45	198	191–249
316 stainless steel	20	...	490
High temperature and refractory metals and alloys			
Beryllium[290–292,295,308]	45	...	...
Beryllium[398]	45	...	...
Beryllium (hot extrusion)[307]	90	...	...
Chromium[323]	45	174	...
Molybdenum:			
Rolled[304,305]	45	191	215–263
Sintered[304,305]	45	216	252–298
Arc cast[305]	45	242	263–308
Niobium[304,305]	45	112	176–181
Niobium[397]	20	...	...
Niobium–2% Zr[306]	45	281	...
Tantalum[304,305]	45	78–120	127–183
Titanium T/AM[304,305]	45	254	262–342
Titanium T/AS[304,305]	45	310	299–324
Titanium D-11[317]	20	...	...
Ti–6Al–4V[317]	45	305	...
Tungsten[304,305]	45	440	450–480
Vanadium[304,305]	45	270	...
Zirconium[304,305]	45	169	190
Zirconium[304,305]	30	170	...
Zircaloy[304,305]	45	292	...
Zircaloy[304,305]	90	265	...

cont.

* Before hydrostatic extrusion; † after hydrostatic extrusion; ‡ mechanical properties (tension, compression) measured in references listed.

Table 4 (cont.)

Material	Die angle, deg	Hardness, HV Billet*	Hardness, HV Product†
Magnesium alloys			
Magnesium[304,305]	45	28	...
Mg–1Al[304,305]	45	36	...
Mg–1Al[304,305]	90	36	...
M/ZTY[304,305]	45	57	76–92
ZW3 (cast)[304,305]	45	66	66–85
AZ91 (cast)[304,305]	45	93	102–116
Mg–Li[416,417]	20	...	...
AZ91–SiCp[416,417]	20	...	...
Aluminum alloys			
99·5% Al[304,305]	45	24	43–50
99·5% Al[304,305]	90	24	43–50
99·5% Al[398]	20	22	60
HE 30 Al (HD44)[304,305]	45	51	...
HE 30 Al (HD44)[304,305]	90	51	...
Al–11Si[304,305]	45	62	80–93
Duralumin II[304,305]	45	71	...
A/FLS[304,305]	45	71	111
AD.1 (99·5 Al)[290–292,295,308]	45	...	...
AD.1 (99·5 Al)[290–292,295,308]	80	...	...
Alloy A (2–2·8 Mg)[290–292,295,308]	45	...	...
Alloy Ak6[290–292,295,308]	45	...	...
1100Al–O[398]	45	...	...
Al (annealed)[307]	90	...	...
Copper alloys			
ERCH[304,305]	45	43	120
ERCH[304,305]	90	43	...
M2 (99·7)[290–292,295,308]	45	...	...
M2 (99·7)[290–292,295,308]	80	...	...
Copper (annealed)[307]	90	...	...
Copper[398]	20	...	...
60/40 brass[304,305]	45	127	181–184
60/40 brass (L62)[290–292,295,308]	80	...	...
Miscellaneous			
Bismuth[304,305]	45	8	4
Yttrium (annealed)[398]	90	...	...
Zinc[398]	20	...	...
NiAl			
extruded at 25 °C[154,164]‡	20	225	725
extruded at 300 °C[154,164]‡	20	225	370–400
Cu–W[391]	...	...	...
X2080Al–SiCp[186,187]‡	20	...	...
Bulk metallic glass (extruded at 300 °C)[417]	20	...	...

* Before hydrostatic extrusion; † after hydrostatic extrusion; ‡ mechanical properties (tension, compression) measured in references listed.

IMS Institute for Materials Science Los Alamos

J.J. Lewandowski and P. Lowhaphandu, International Materials Reviews, Vol.43, No.4, 1998.

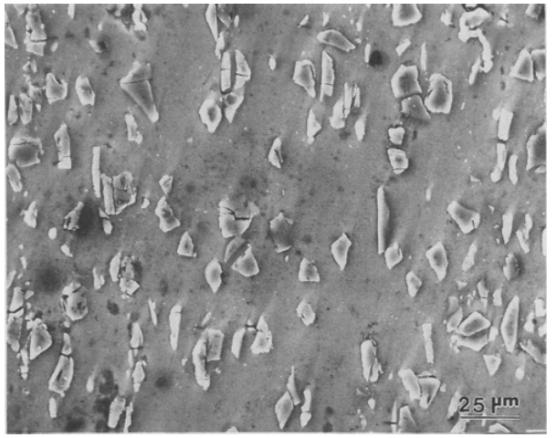

Fig. 11—Micrograph showing cracked SiC_p on the surface of the 13 μm-UA specimen after about 6.3 pct global plastic strain, ε_{gpl}.

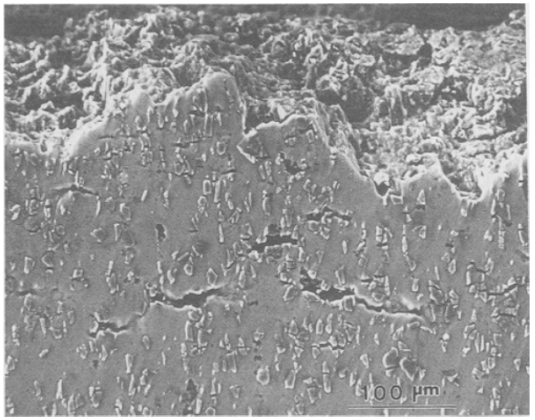

Fig. 16—Micrograph showing area near fracture surface for the 13 μm-UA specimen. Fracture surface is located at top.

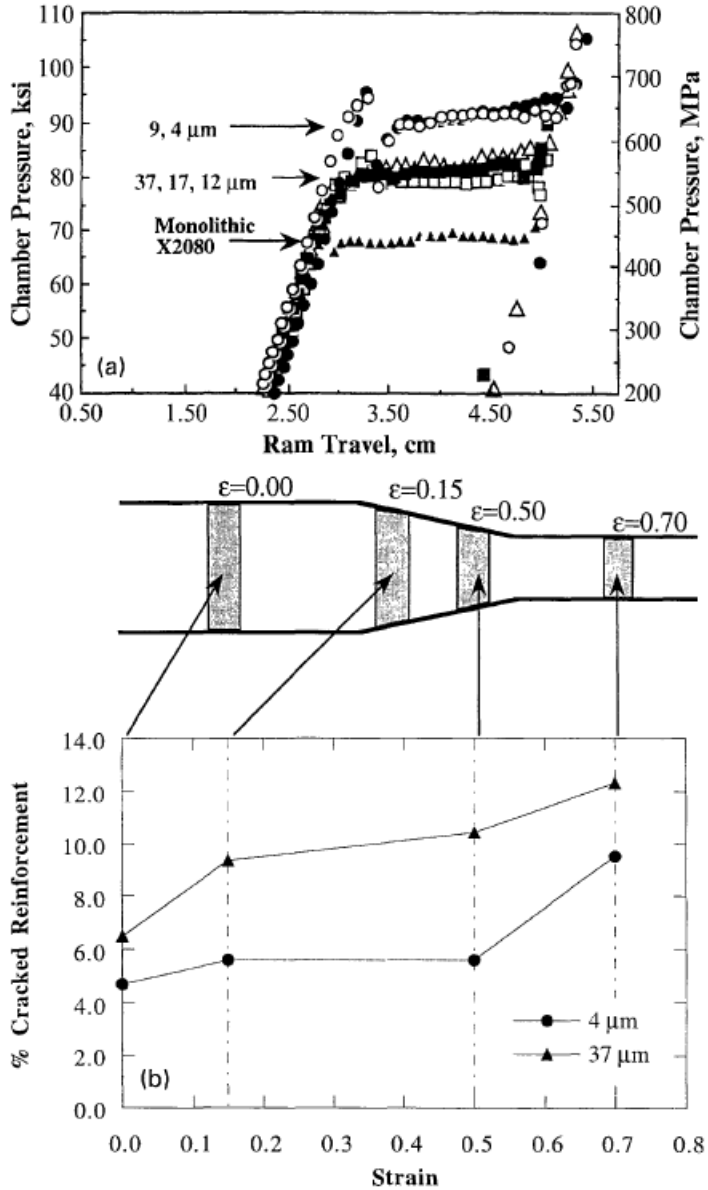

51 ***a*** **Effects of reinforcement size on chamber pressure *v.* ram travel for hydrostatic extrusion of aluminium composites: addition of reinforcement and decreasing reinforcement size increased extrusion pressure and *b* damage assessment as function of extrusion strain for hydrostatically extruded materials[186,187]**

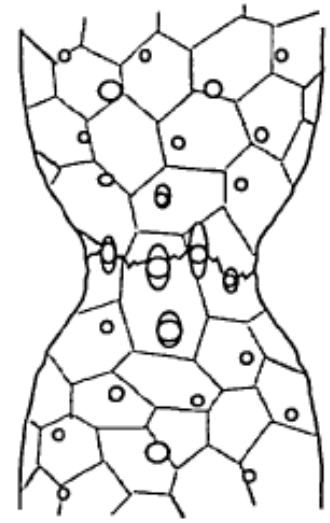

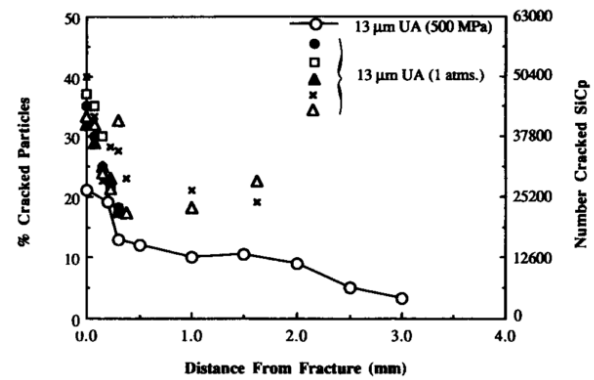

Fig. 29—Effects of tension testing with 500 MPa confining pressure on the amount of cracked SiC_p as a function of the distance from the fracture surface of the 13 μm UA material. Data from Fig. 14 on identical specimens tested to failure at atmospheric pressure are included for comparison.

Grow, A.L. and Lewandowski, J.J. (1995) SAE Transactions, Paper #950260.

IMS Institute for Materials Science Los Alamos

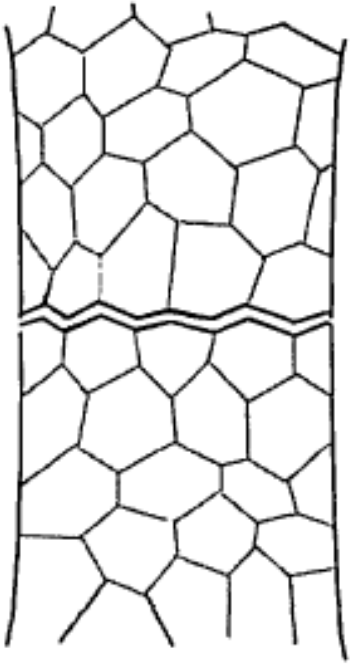

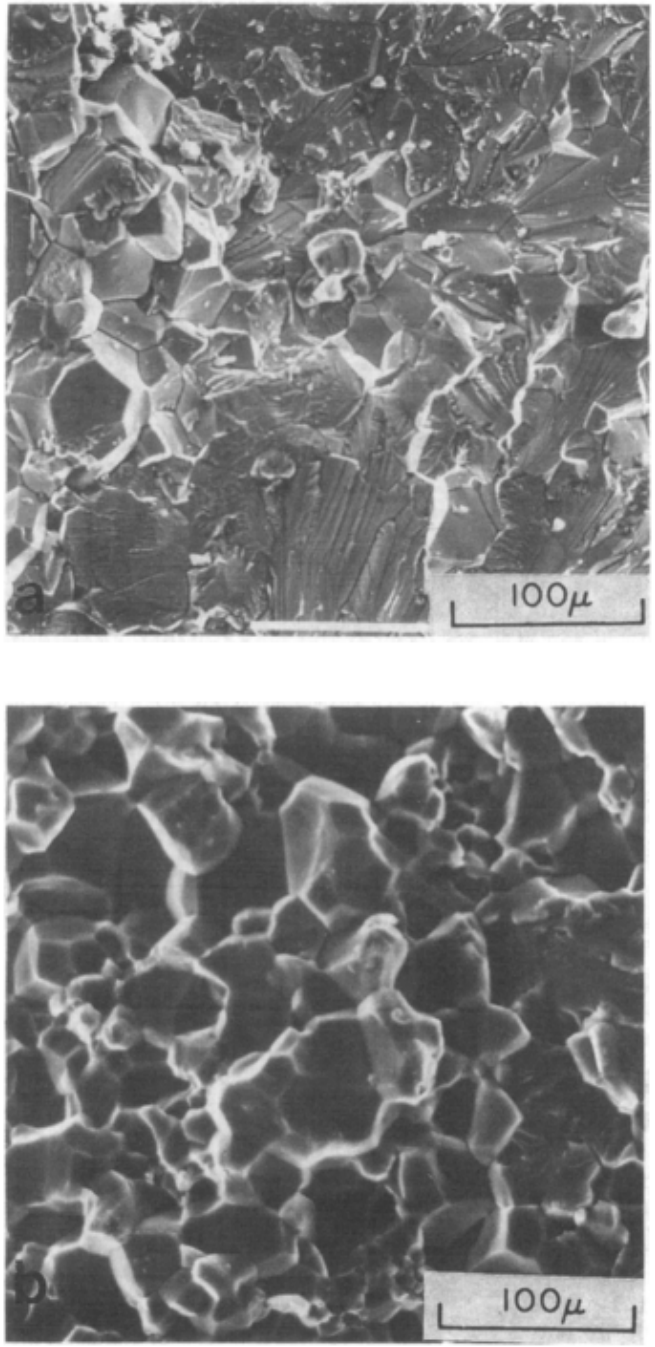

Fig. 12—SEM micrographs of the fracture surfaces of cast NiAl specimens tested at (*a*) 0.1 MPa and (*b*) 500 MPa pressure.

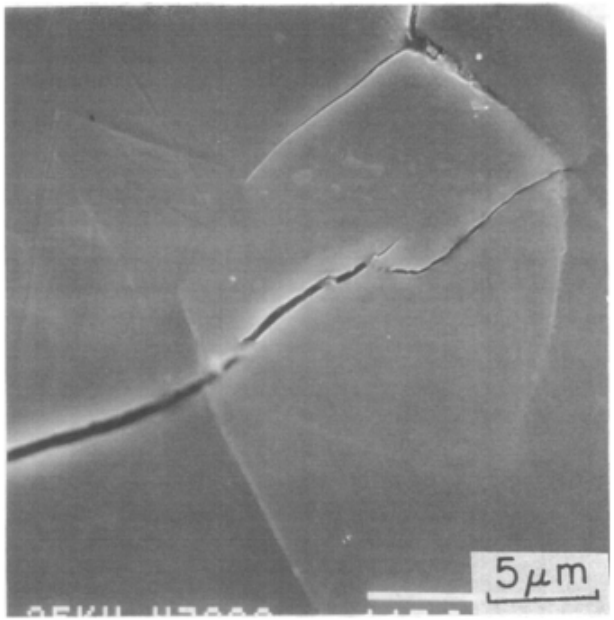

Fig. 9—SEM micrograph of TG microcrack on the external surface of the sample tested in tension at 500 MPa to 10 pct strain. Loading axis is vertical.

R.W. Margevicius and J.J. Lewandowski, Metall. Mat. Trans. A **25**, 1457 (1994).

IMS Institute for Materials Science Los Alamos

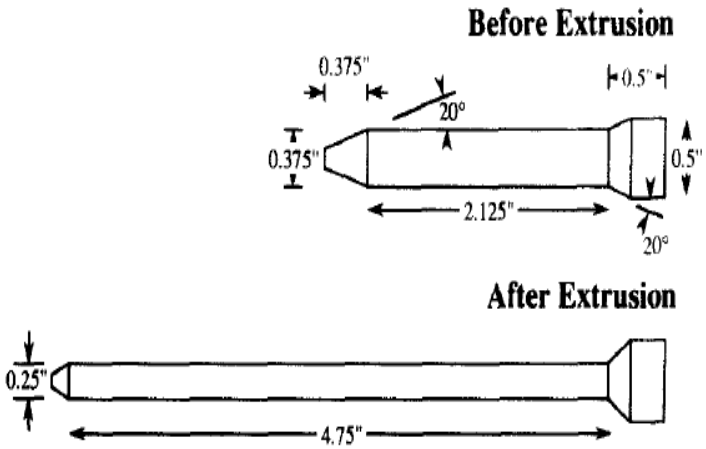

Fig. 2. Dimensions of extrusion billet prior to and following hydrostatic extrusion.

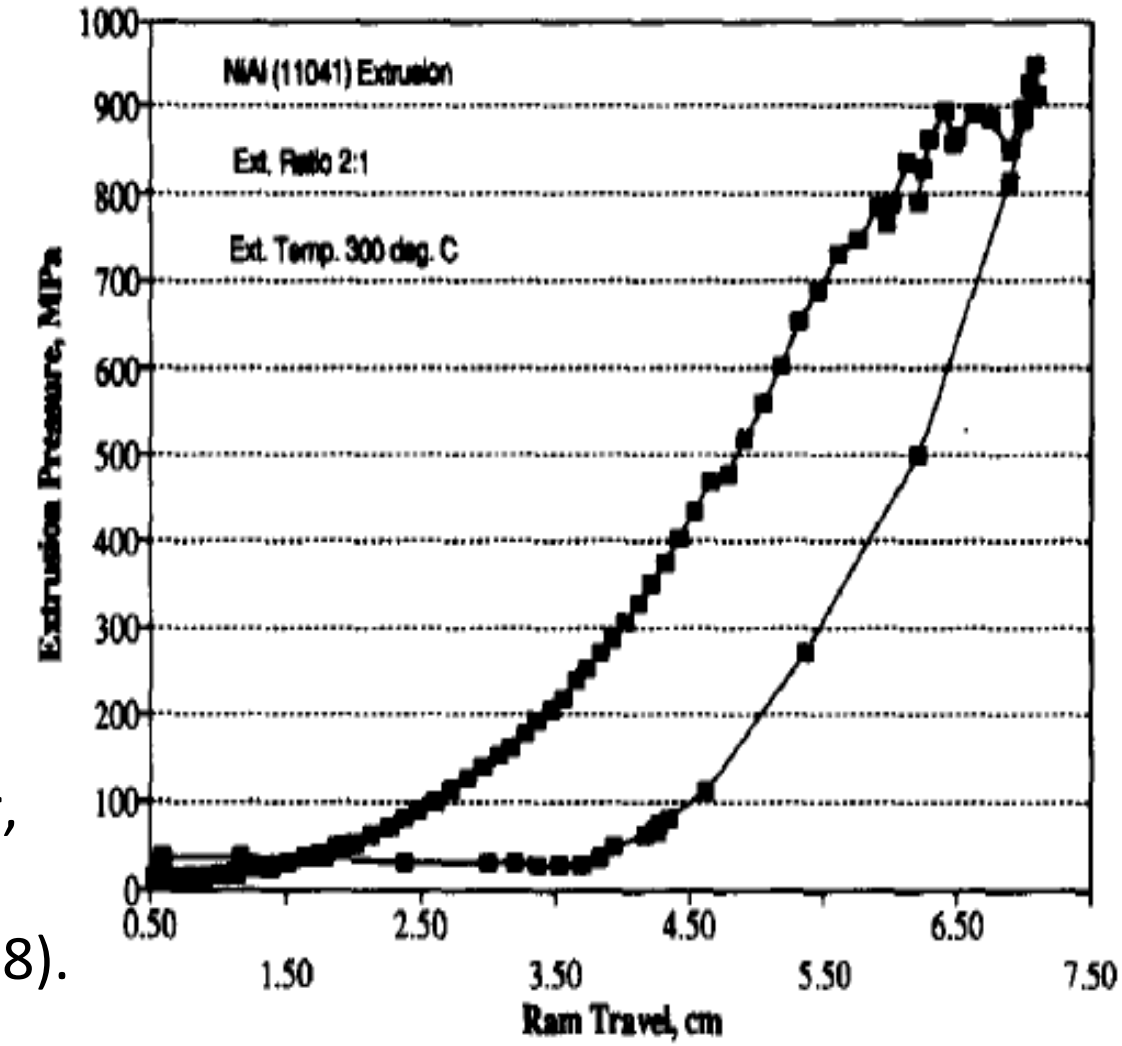

J.J. Lewandowski, B. Berger, J.D. Rigney, and N. Sunil, Philos. Mag. A **78**, 643 (1998).

Fig. 4. Chamber pressure versus ram displacement curve showing increase in pressure as a function of ram travel. Extrusion is indicated by the abrupt change in slope.

IMS Institute for Materials Science Los Alamos

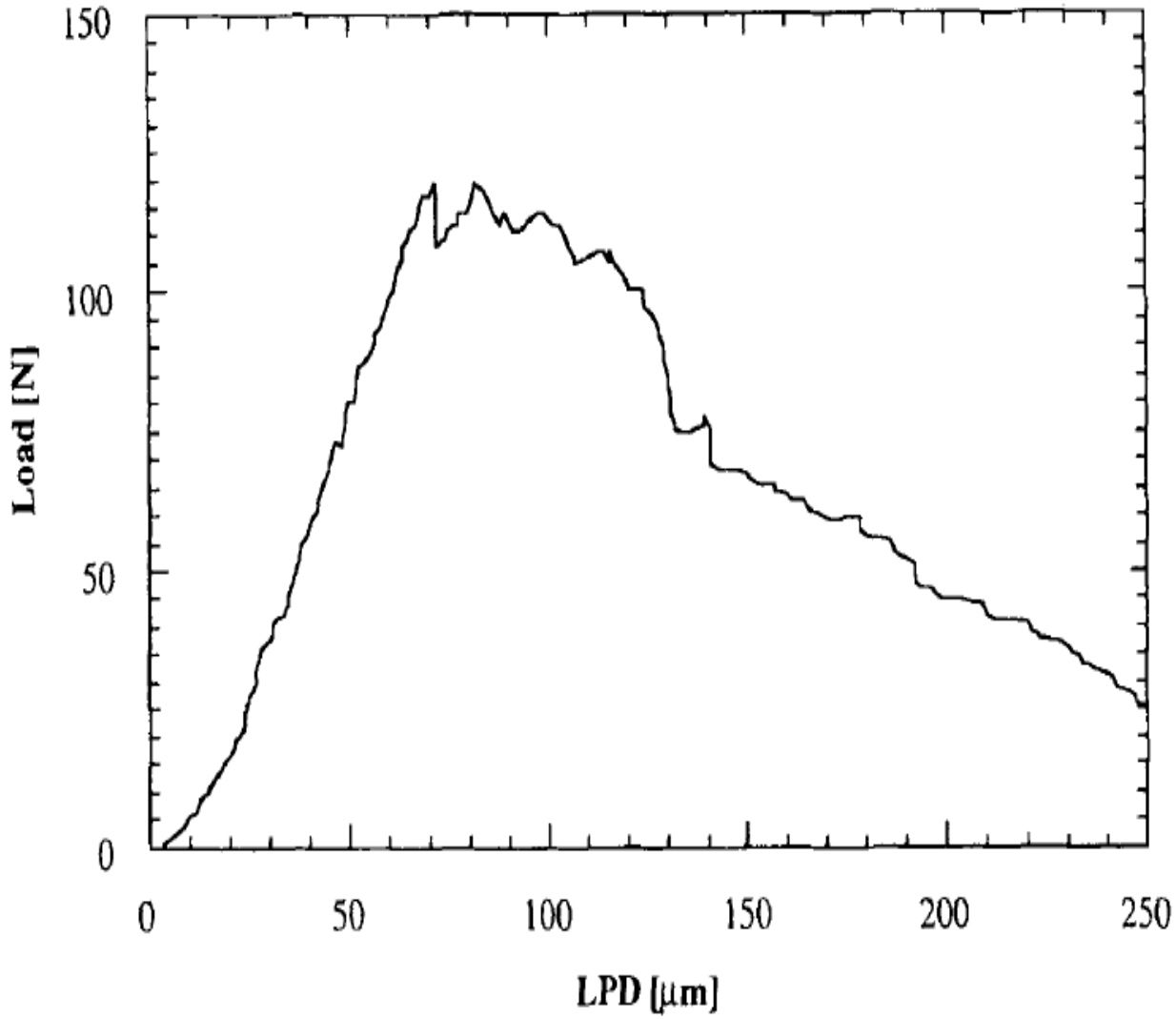

Figure 3. Typical load–load displacement trace from the fracture toughness test on the hydrostatically extruded NiAl.

J.J. Lewandowski, B. Berger, J.D. Rigney, and N. Sunil, Philos. Mag. A **78**, 643 (1998).

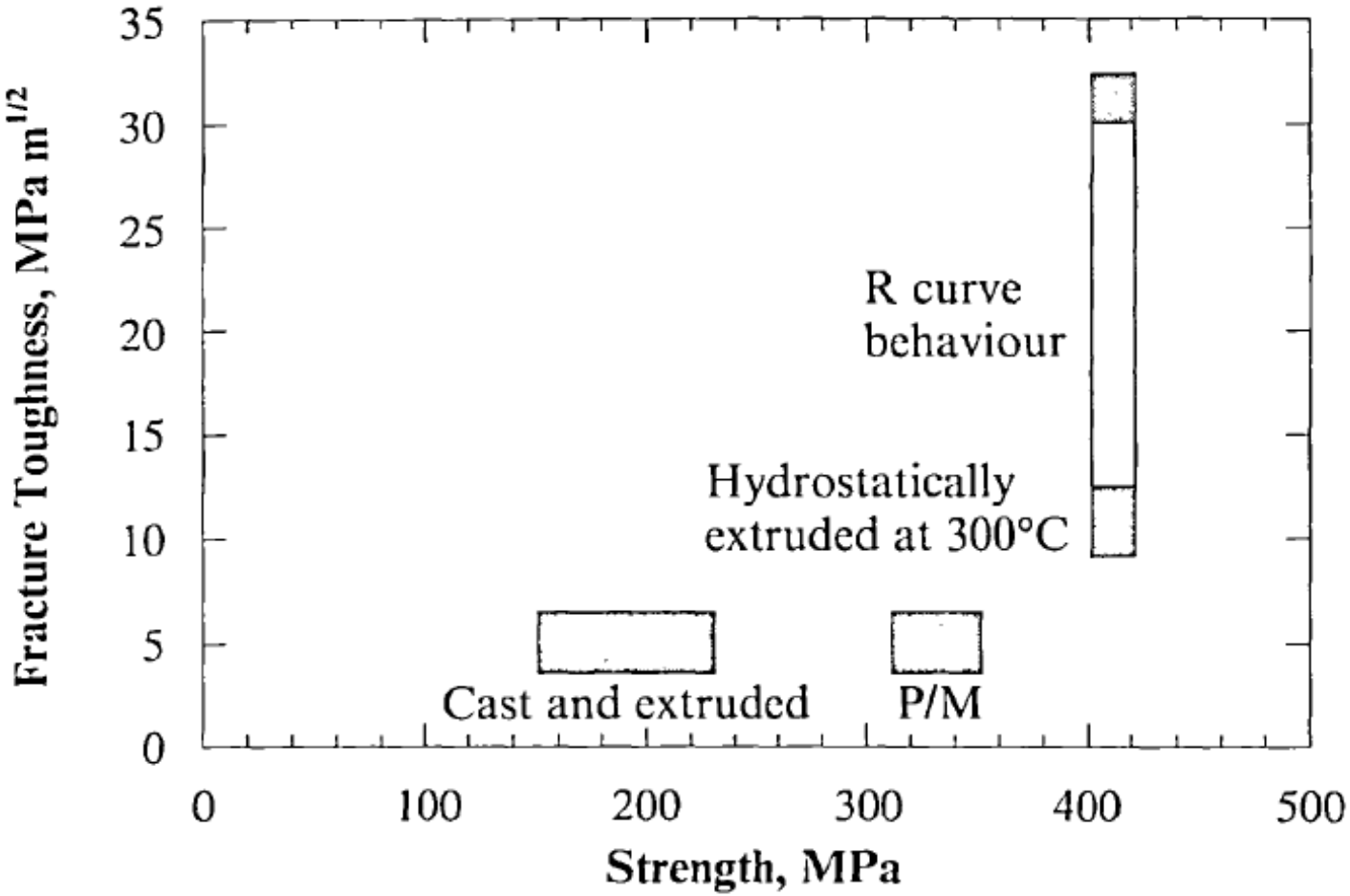

52 Fracture toughness–strength combination of hydrostatically extruded NiAl (Ref. 154)

J.J. Lewandowski, B. Berger, J.D. Rigney, and N. Sunil, Philos. Mag. A **78**, 643 (1998).

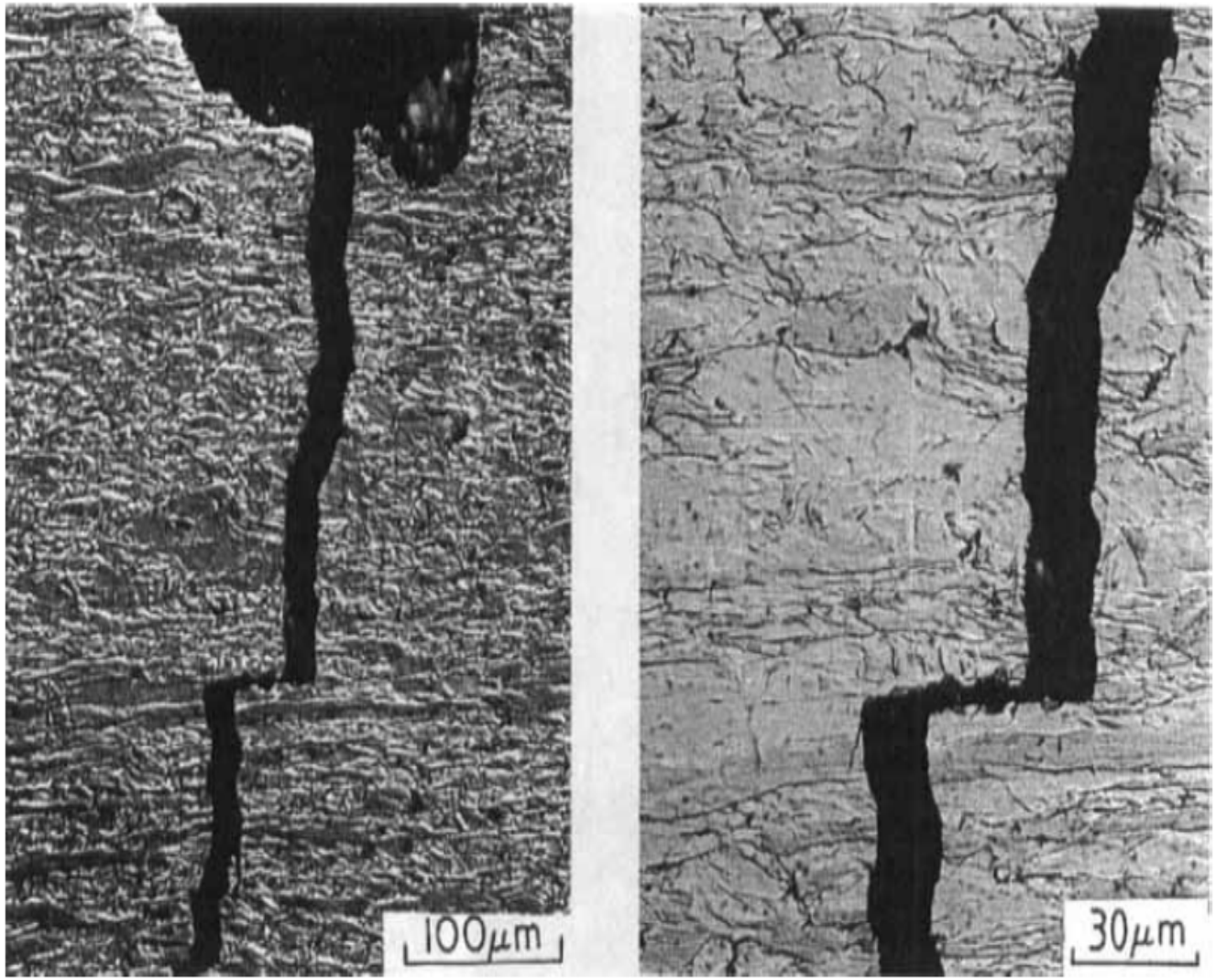

Figure 6. Low-magnification Nomarski optical view of notch-tip region in a toughness test of hydrostatically extruded NiAl. The higher-magnification view shows detail of crack-tip bifurcation along the grain boundary parallel to the extrusion direction.

J.J. Lewandowski, B. Berger, J.D. Rigney, and N. Sunil, Philos. Mag. A **78**, 643 (1998).

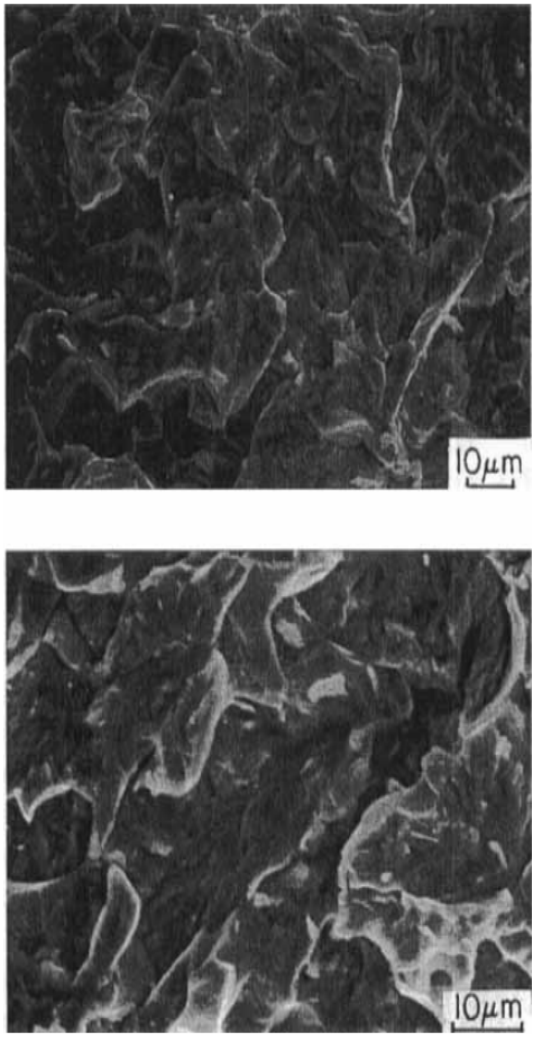

Figure 5. Scanning electron microscopy fractography of the notch toughness tests on hydrostatically extruded NiAl showing transgranular quasicleavage fracture.

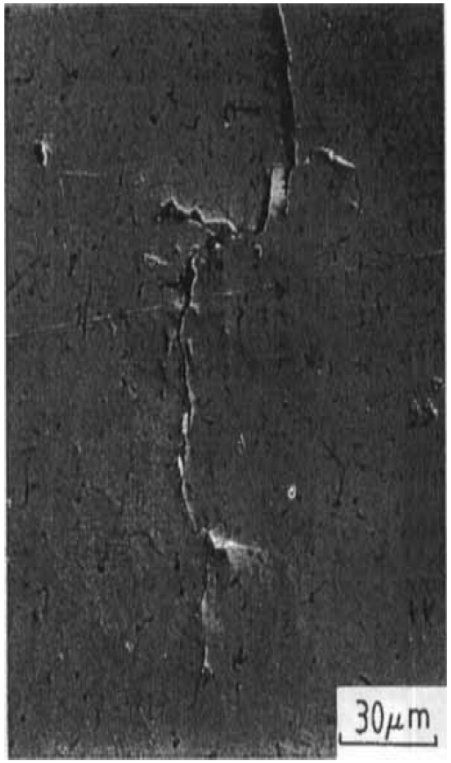

Figure 4. Optical micrograph of arrested crack tip in notch toughness test of hydrostatically extruded NiAl showing plasticity at the crack tip and crack-tip bifurcation.

IMS Institute for Materials Science Los Alamos

J.J. Lewandowski, B. Berger, J.D. Rigney, and N. Sunil, Philos. Mag. A **78**, 643 (1998).

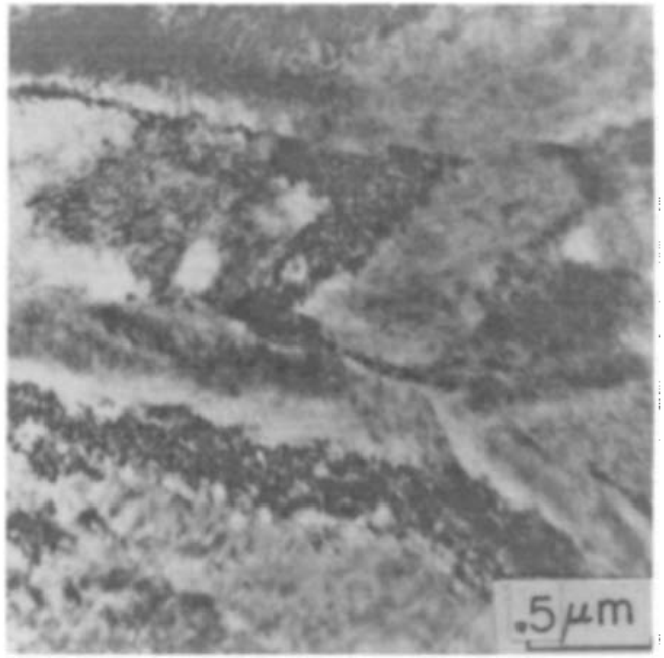

Figure 5. TEM micrograph showing extensive deformation and subgrain formation after hydrostatic extrusion at 573K.

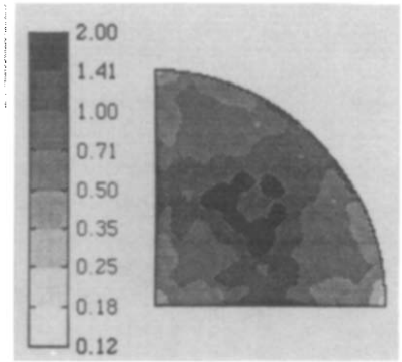

Figure 2. Initial texture before hydrostatic extrusion showing a partially recrystallized {111} fiber texture.

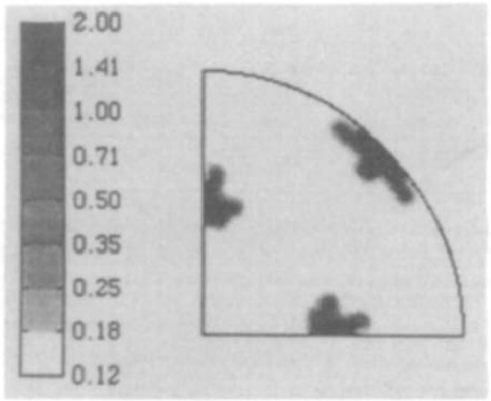

Figure 4. Inverse pole figure for NiAl hydrostatically extruded at 573 K.

IMS Institute for Materials Science Los Alamos

R.W. Margevicius and J J. Lewandowski, Scr. Metall. Mater. **29**, 1651 (1993).

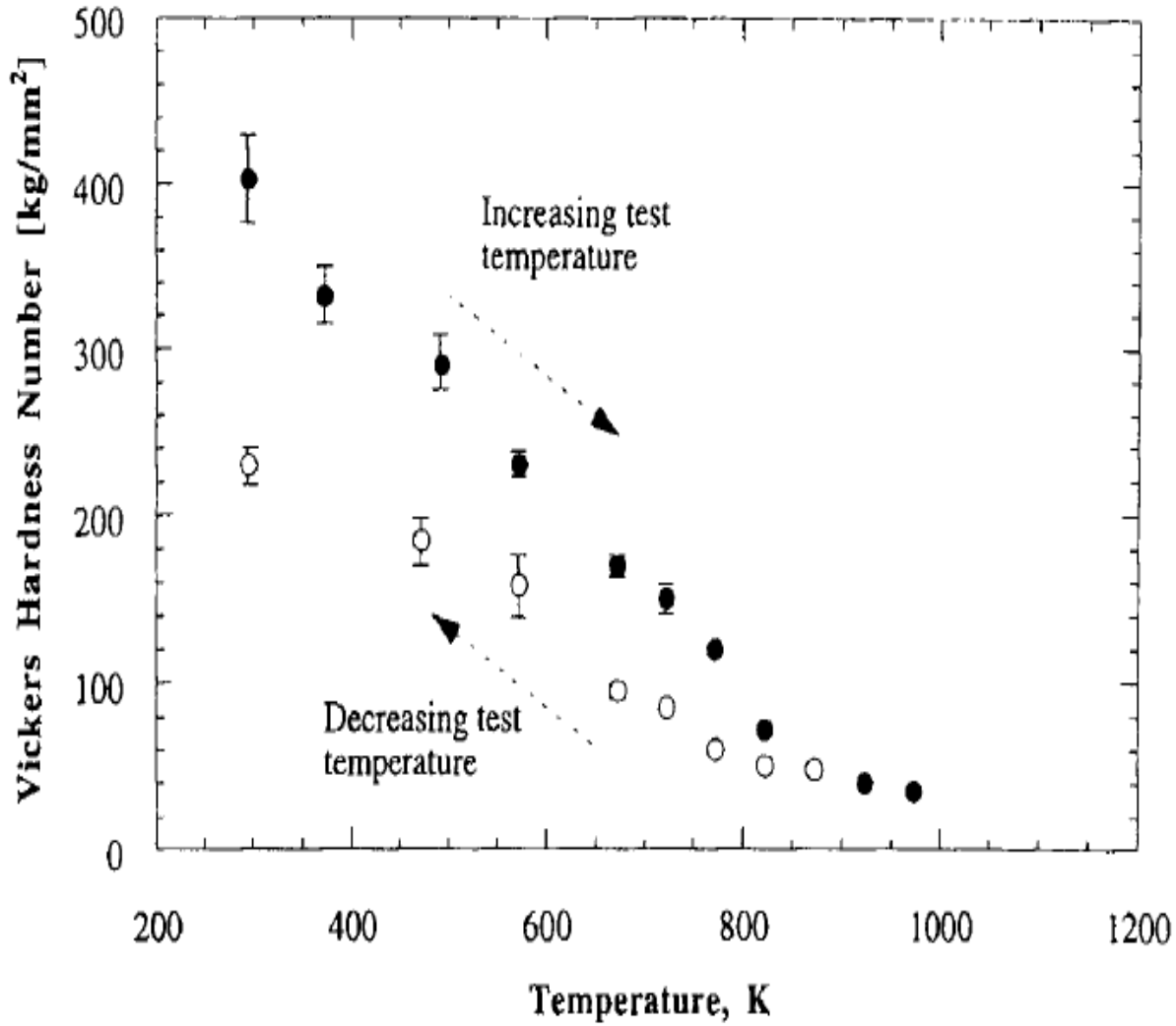

Figure 1. Hot microhardness results showing the effects of increasing temperature and subsequent decreasing temperature of hydrostatically extruded NiAl.

IMS Institute for Materials Science Los Alamos

J.J. Lewandowski, B. Berger, J.D. Rigney, and N. Sunil, Philos. Mag. A **78**, 643 (1998).

Table 1. Effects of processing conditions on mechanical properties of NiAl.

Material identification and processing	Microhardness (1 kg load) (HV)	Compressive yield strength (MPa)	Notch toughness (MPa $m^{1/2}$)	Fractography	Comments
Cast and conventionally extruded at 1173 K (16:1 ratio)	225 ± 10	225 ± 25	5.5 ± 0.1	Integranular and transgranular cleavage	Linear load–displacement trace
Hydrostatically extruded at 298 K (2:1 ratio)	725 ± 25	N/A	N/A	N/A	Billet cracked
Hydrostatically extruded at 573 K (2:1 ratio)	370[a] ± 25	400[a]	10.2[a]	Transgranular	R curve K_{max} = 28.5 MPa $m^{1/2}$
	370 ± 20	400	11.0	Quasicleavage	R curve K_{max} = 29.0 MPa $m^{1/2}$
	400 ± 25	420	12.8	Quasicleavage	R curve K_{max} = 28.0 M Pa $m^{1/2}$
	400 ± 20	420	13.0	Quasicleavage	R curve K_{max} = 28.5 MPa $m^{1/2}$
Hydrostatically extruded at 573 K (2:1 ratio) annealed at 973 K for 1 h and then furnace cooled	215 ± 15	N/A	5.1	Intergranular and transgranular cleavage	Linear load–displacement trace

[a] Annealed at 673 K for 2 h and then furnace cooled.

IMS Institute for Materials Science Los Alamos

J.J. Lewandowski, B. Berger, J.D. Rigney, and N. Sunil, Philos. Mag. A **78**, 643 (1998).

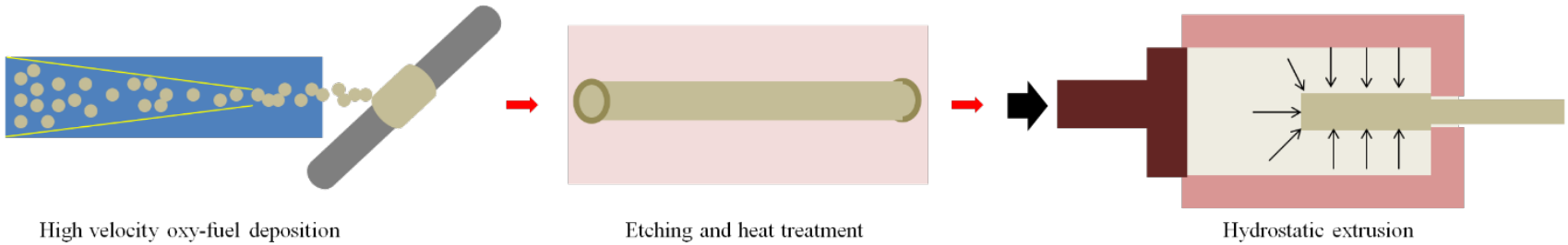

J Bobanga et al (2015)

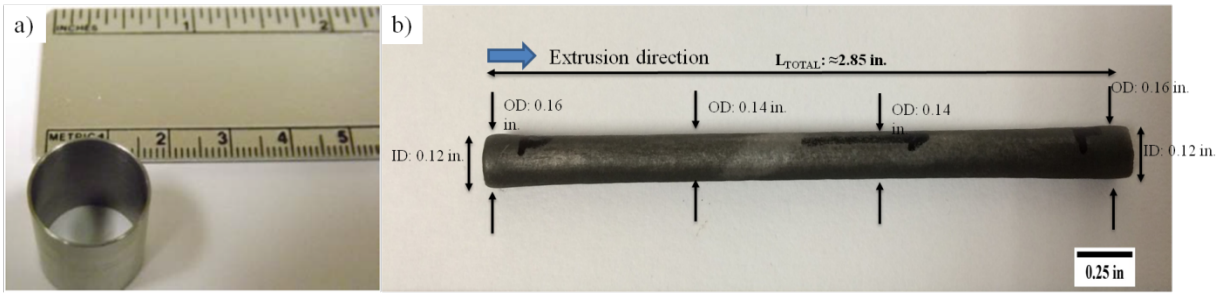

E Aydogan et al (2015)

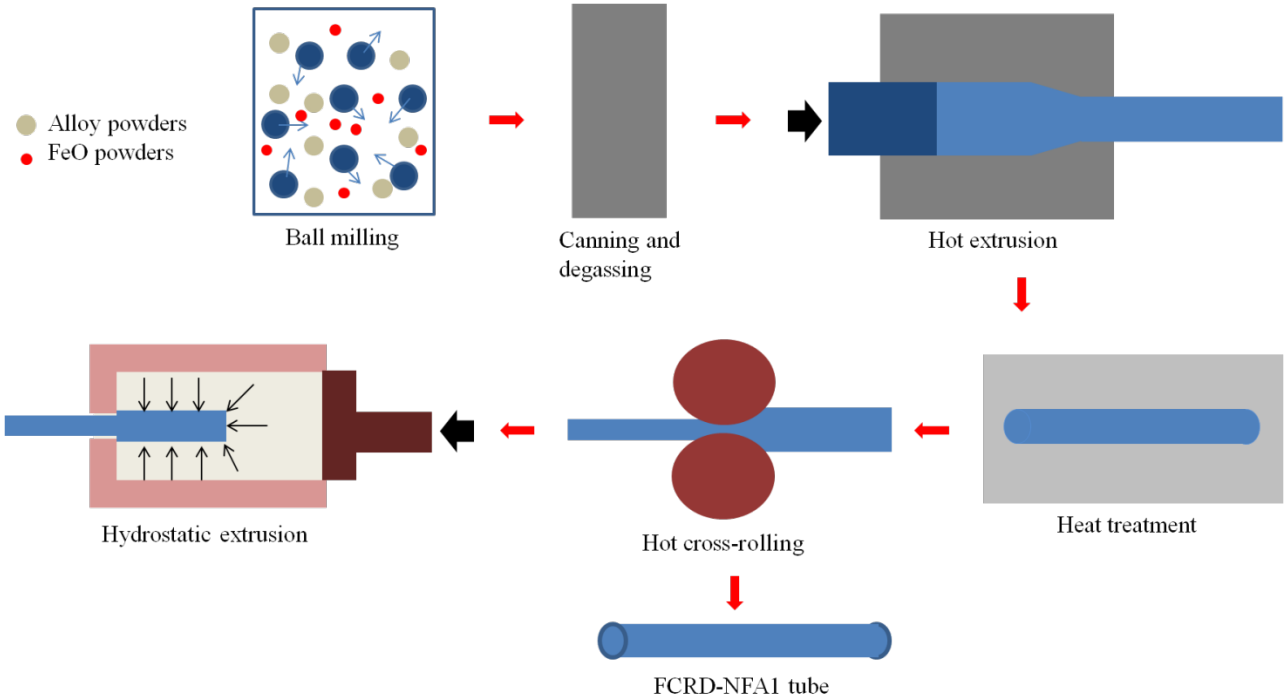

IMS Institute for Materials Science Los Alamos

ODS COMPOSITE TUBE EXTRUSION

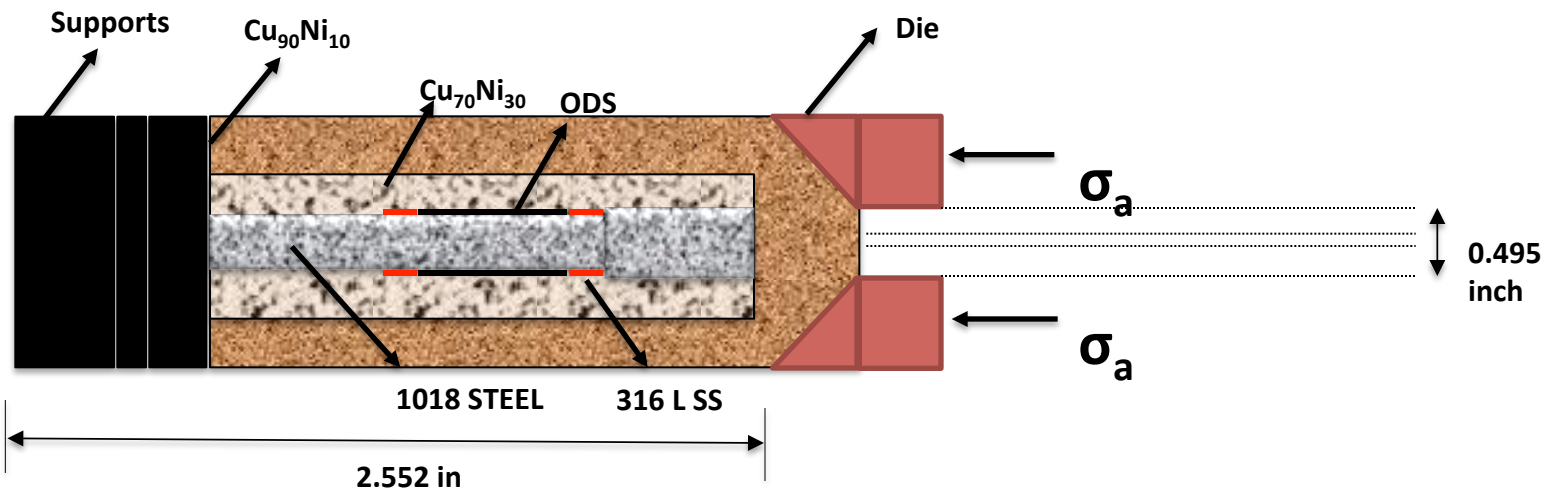

CHAMBER ASSEMBLY BEFORE EXTRUSION

J Bobanga et al (2015)

1. EXTRUSION TEMP: 1500F
2. RAM SPEED: 0.5 in/min
3. SOAK TIME: 10 min
4. OVERALL EXTRUSION:
5. ER: 4:1, 45 DEG TAPER DIE

IMS Institute for Materials Science Los Alamos

ODS, STEEL MANDREL, $Cu_{70}Ni_{30}$ CLADDING AND $Cu_{90}Ni_{10}$ CLADDING ASSEMBLY PRIOR TO EXTRUSION

IMS Institute for Materials Science Los Alamos

J Bobanga
et al (2015)

FASTER COOLING

SLOWER COOLING

Chamber Assembly after Extrusion

Die and Billet Readied for Die Removal

IMS Institute for Materials Science Los Alamos

J Bobanga et al (2015)

ODS TUBE

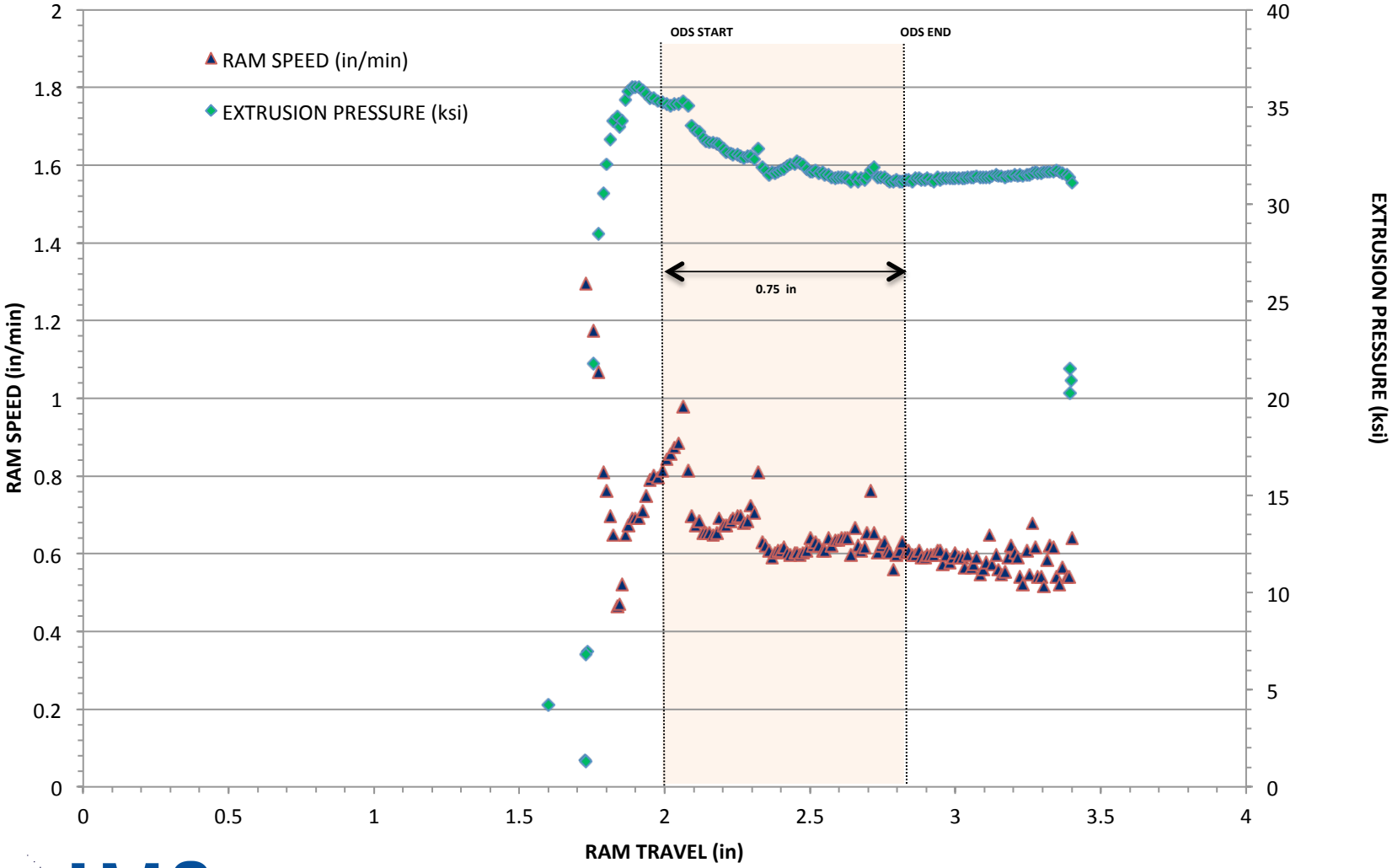

IMS Institute for Materials Science Los Alamos

J Bobanga
et al (2015)

EXTRUDED ODS TUBE AND CLADDING

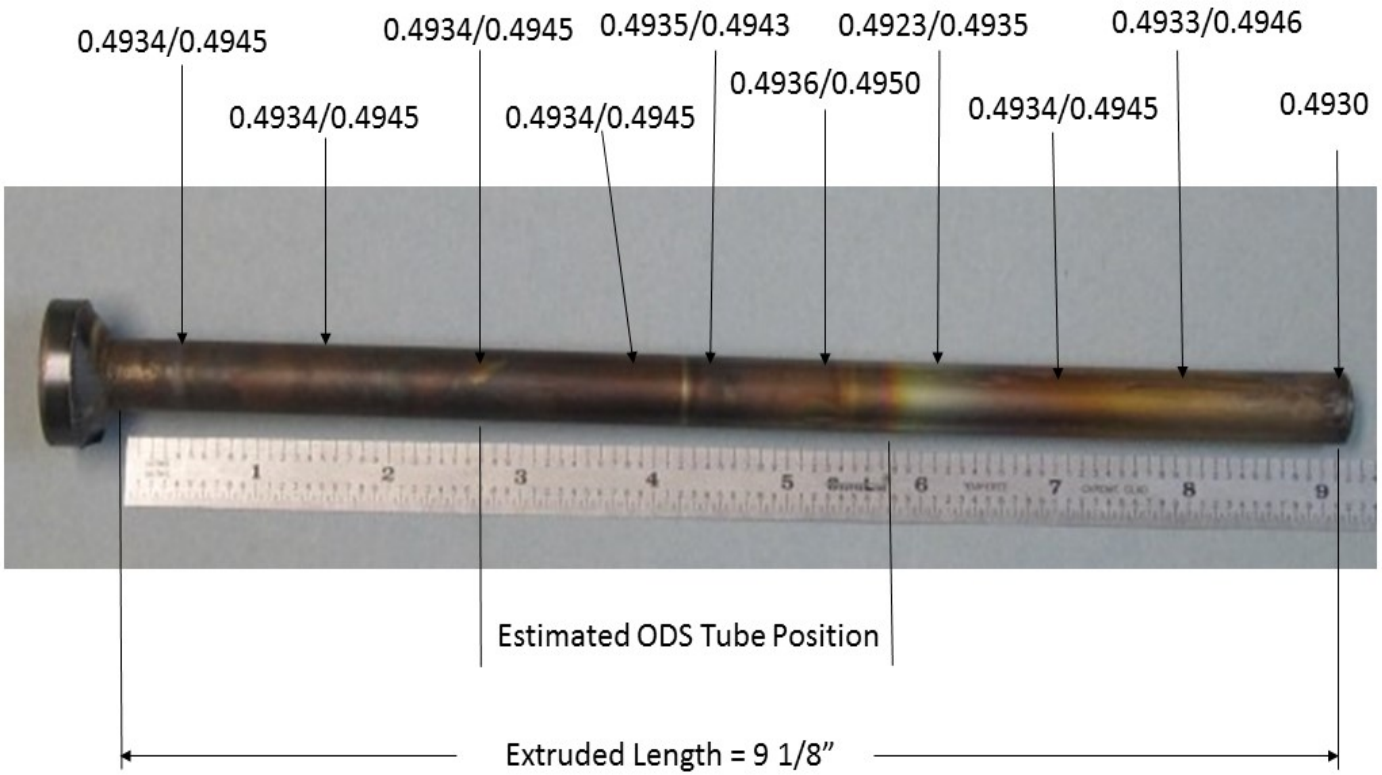

ODS TUBE EXTRUSION CWRUEXTR.108 – 10/07/2014

IMS Institute for Materials Science Los Alamos

J Bobanga
et al (2015)

EXTRUDED ODS TUBE

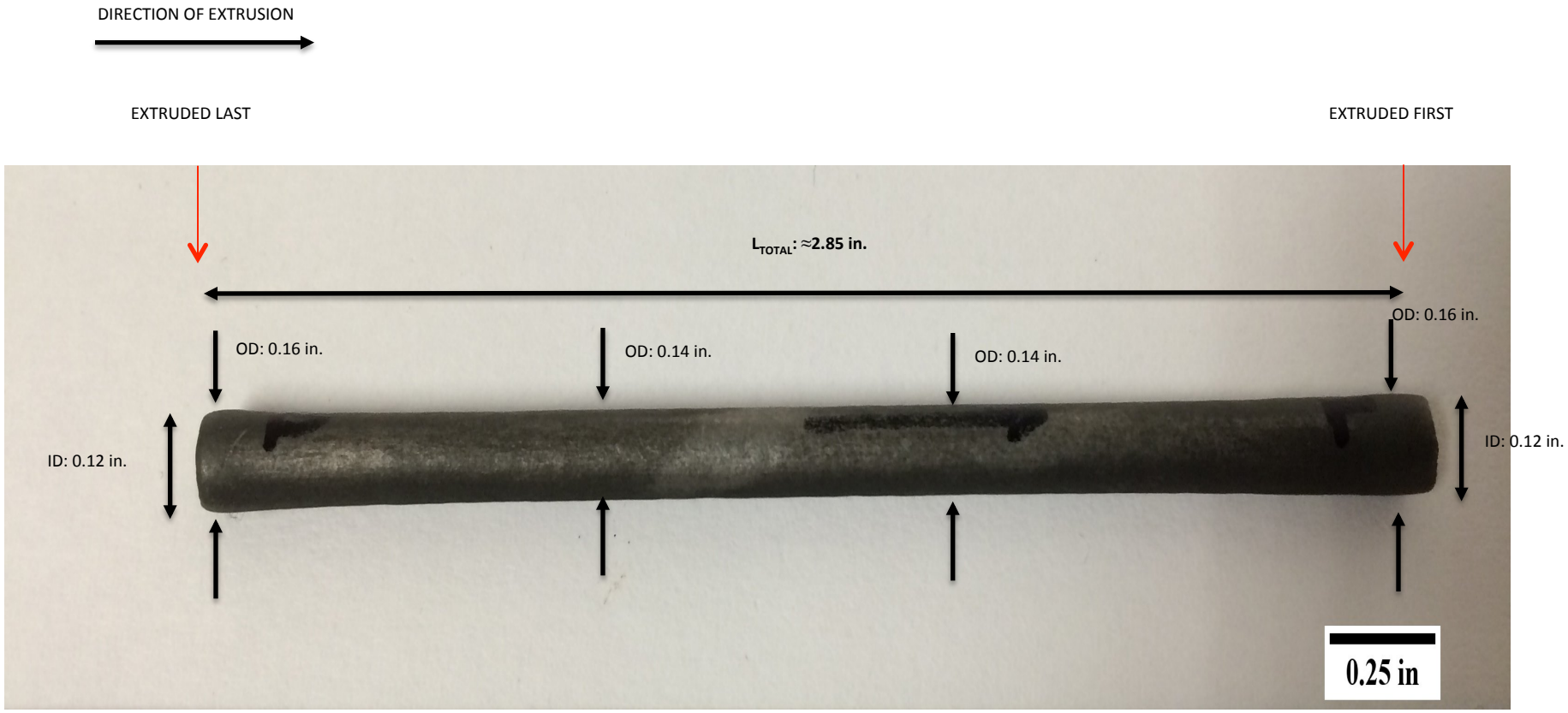

Fig. 1 Overall Image of Extruded ODS Tube After Etching(ER: 4:1, 45° angle die, 4.2 in/min product rate, 815°C extrusion temperature)

IMS Institute for Materials Science Los Alamos

J Bobanga
et al (2015)

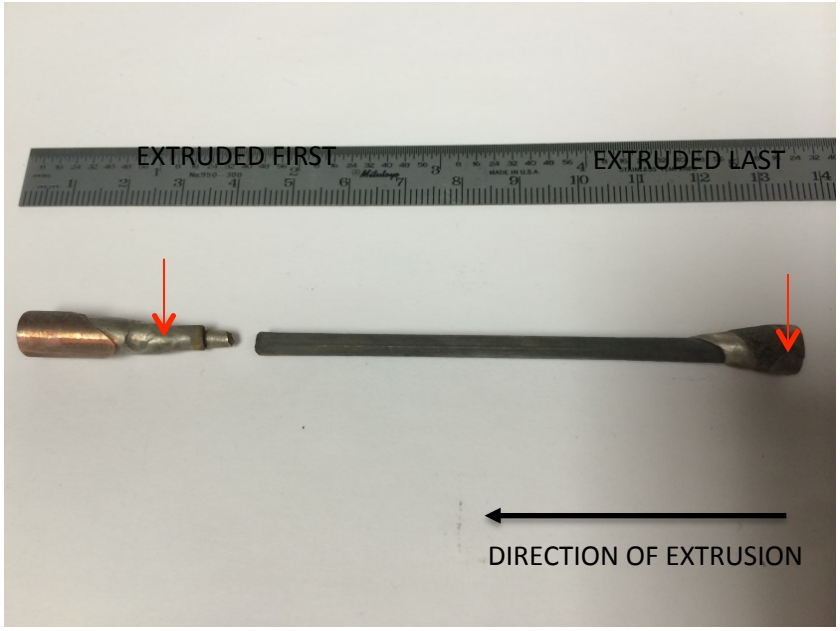

CHEMICAL MILLING OF ODS COMPOSITE
(3-day at 23% Nitric Acid)

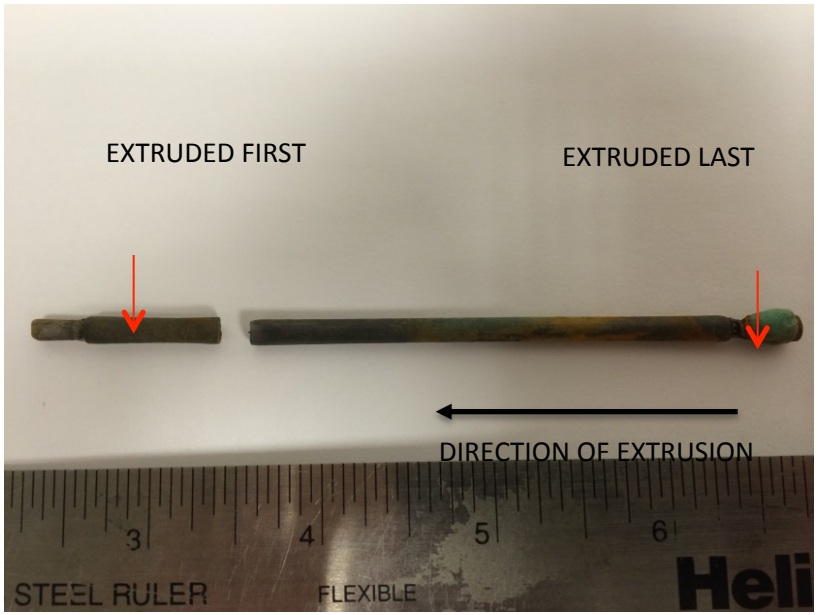

CHEMICAL MILLING OF ODS COMPOSITE
(6-day Total at 23% Nitric Acid)

IMS Institute for Materials Science Los Alamos

J Bobanga
et al (2015)

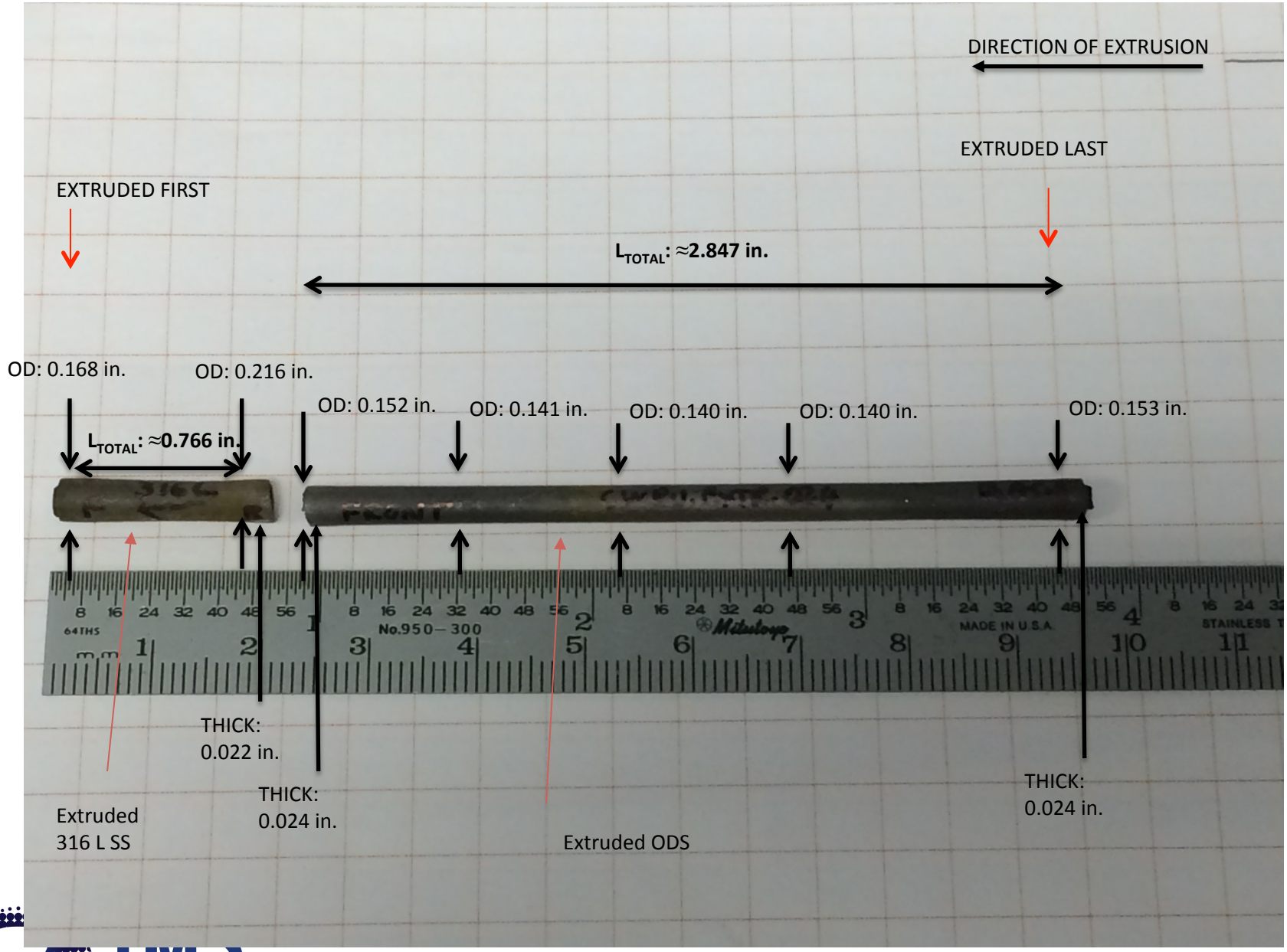

Extruded ODS and 316L SS Tubes
(ER: 4:1, 45° angle die, 0.5 in/min ram speed, 815°C extrusion temperature)

PROGRESSION OF ODS EXTRUSIONS

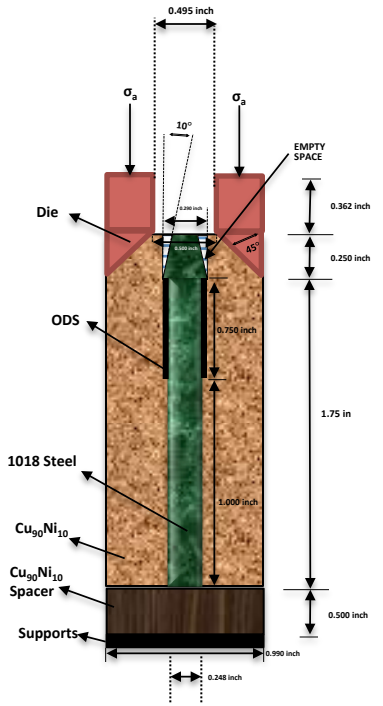

DRAWING NOT TO SCALE

1. CWRU.EXTR.023 19 AUG 14
2. EXTRUSION TEMP: 815°C
3. RAM SPEED: 0.5-0.7 in/min
4. SOAK TIME: 10 min
5. OVERALL EXTRUSION: 7.2 inch
6. ER: 4:1, 45 DEG TAPER DIE
7. See Separate Attachment

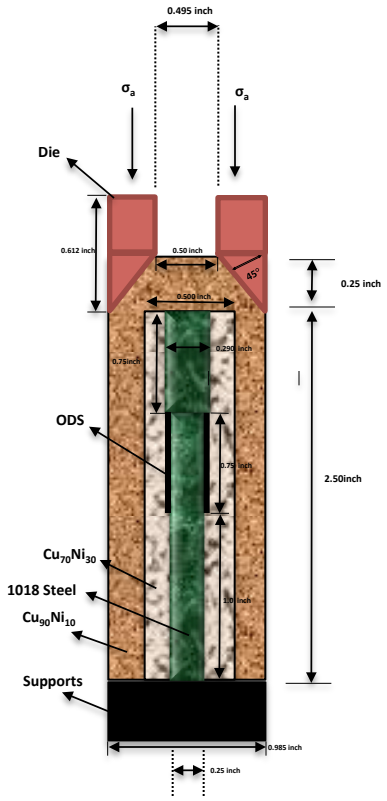

DRAWING NOT TO SCALE

1. CWRU.EXTR.108 IE 7 OCT 14
2. EXTRUSION TEMP: 815°C
3. PRODUCT RATE: 4.0 in/min
4. SOAK TIME: 10-15 min
5. OVERALL EXTRUSION: 9 1/8 inch
6. ER: 4:1, 45 DEG TAPER DIE
7. See Separate Attachment

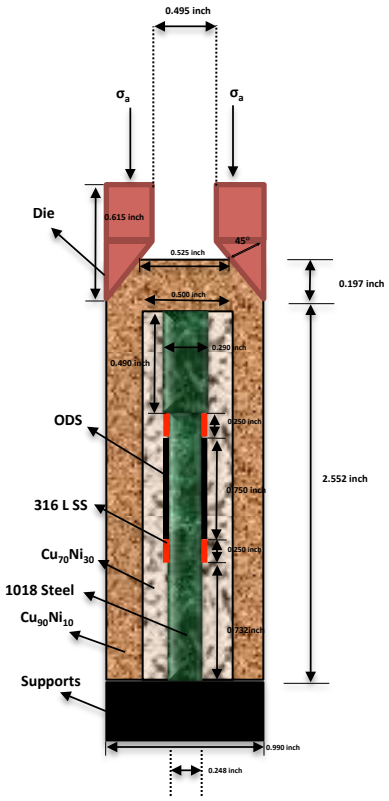

DRAWING NOT TO SCALE

1. CWRU.EXTR.024 26 NOV 14
2. EXTRUSION TEMP: 815°C
3. RAM SPEED: 0.5 in/min
4. SOAK TIME: 20 min
5. OVERALL EXTRUSION: 7 inch
6. ER: 4:1, 45 DEG TAPER DIE
7. See Separate Attachment

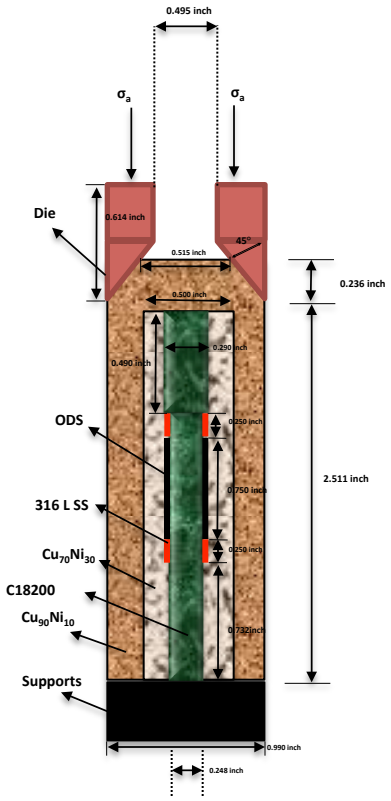

DRAWING NOT TO SCALE

1. CWRU.EXTR.025 31 JUL 15
2. EXTRUSION TEMP: 815°C
3. RAM SPEED: 4.5 in/min
4. SOAK TIME: 15 min
5. OVERALL EXTRUSION: 7 inch
6. ER: 4:1, 45 DEG TAPER DIE
7. See Separate Attachment

IMS Institute for Materials Science Los Alamos

J Bobanga et al (2015)

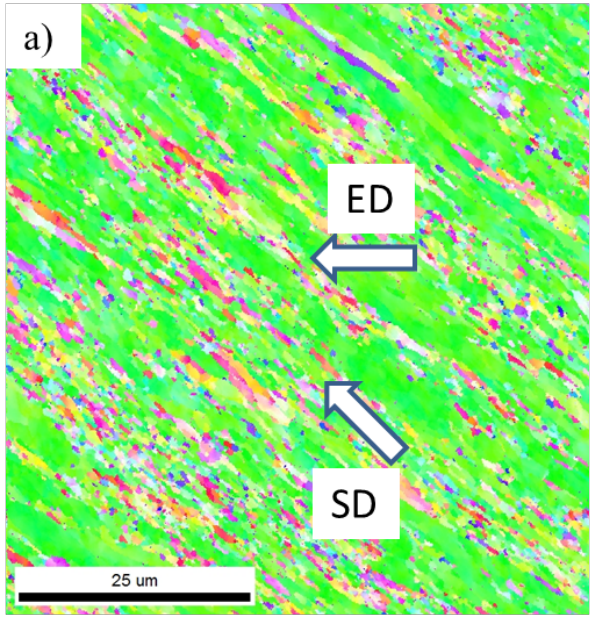

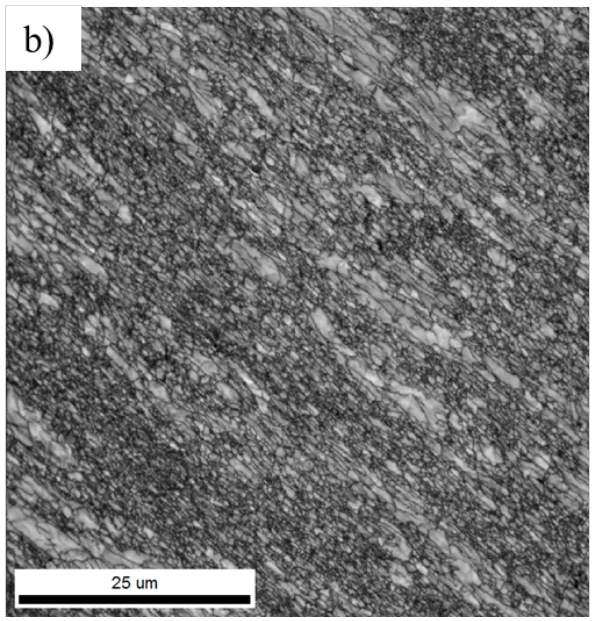

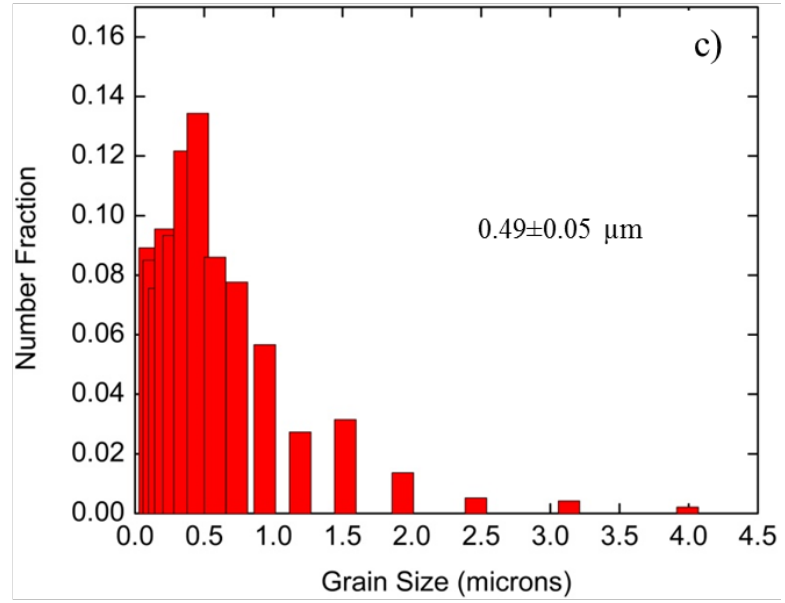

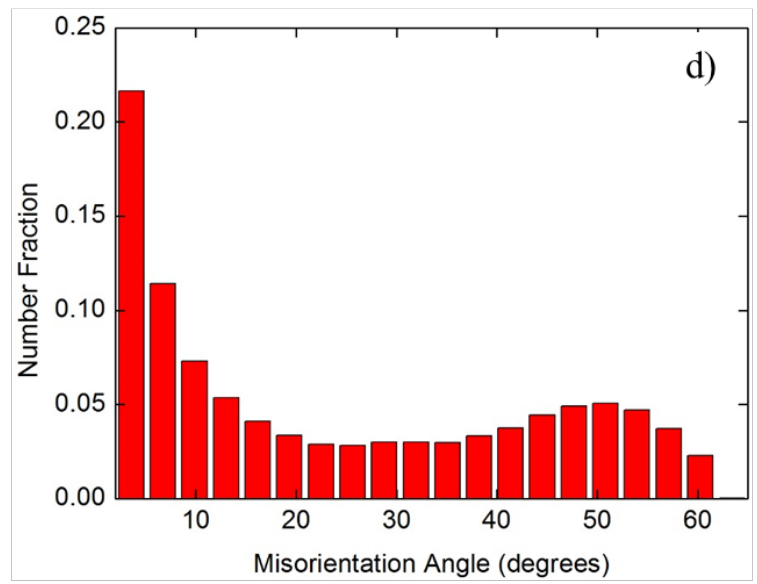

IMS Institute for Materials Science Los Alamos

E Aydogan
et al (2015)

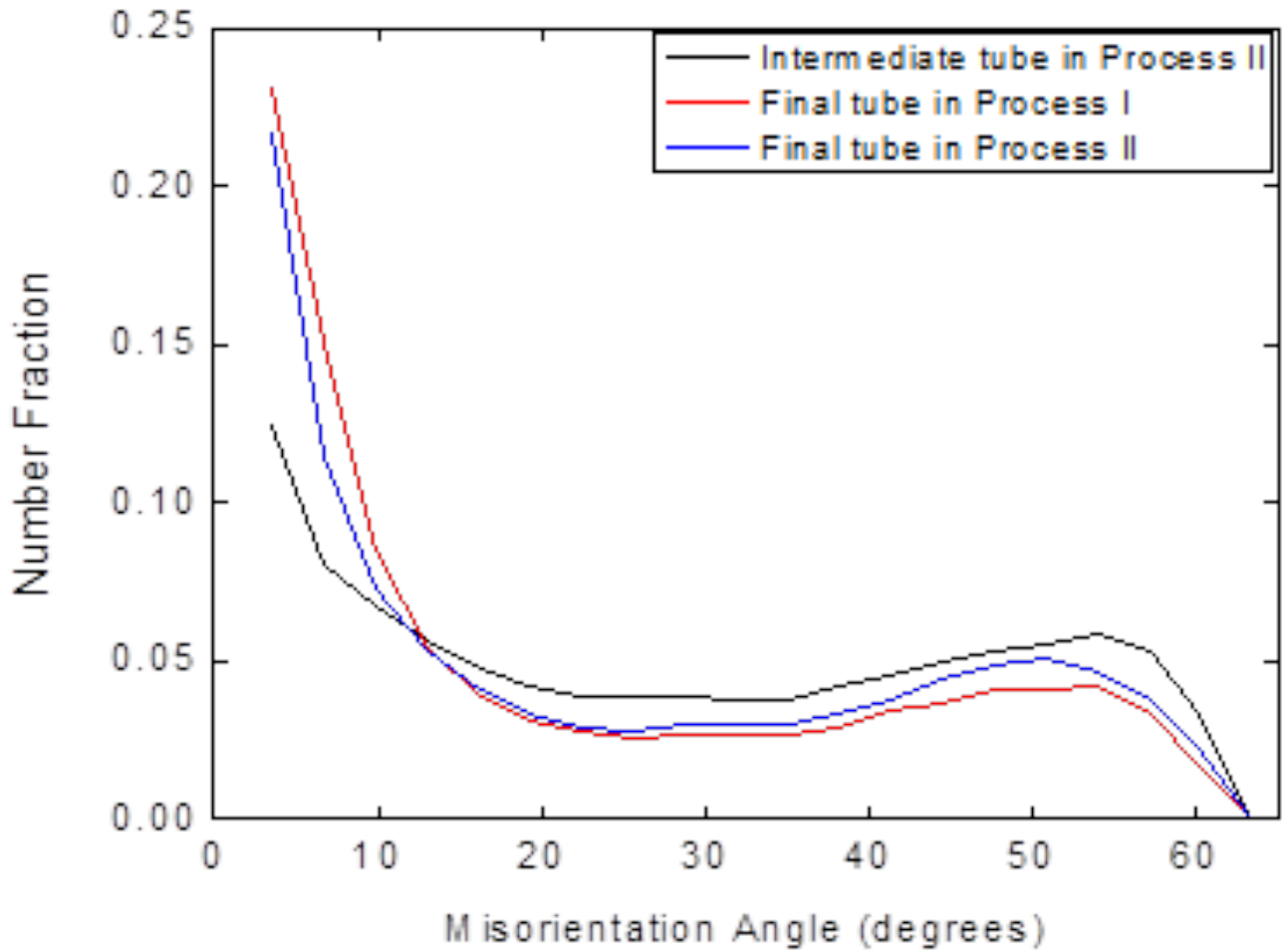

IMS Institute for Materials Science Los Alamos

E Aydogan
et al (2015)

Summary

- High Pressure Testing Rigs
  - Pressure Media: Gas, Oil
  - Internal Load Cell, Pressure Measurement
- Pressure Effects on Flow of Metallic Alloys
  - Yielding
    - Cubic Systems
    - Non-Cubic Systems
    - Particle-containing systems
  - UTS

- Pressure Effects on Fracture of Metallic Alloys
    - Fracture Micro-mechanisms
    - Pressure Effects on Ductility/Fracture
- Pressure Effects on Composites, Intermetallics
  - Flow
    - Ductility/Fracture
    - Pressure and Temperature Effects
        - Implications on Deformation Processing
- Hydrostatic Extrusion
    - Concept
    - Examples (Composites, NiAl)
    - ODS Tubes?
        - Billet Design, Initial Results

IMS Institute for Materials Science Los Alamos